Journal of Medicinal Chemistry

ARTICLE

pubs.acs.org/jmc

# Discovery of Potent and Selective Inhibitors of Human Platelet-Type 12- Lipoxygenase

Victor Kenyon,[||,⊥,#] Ganesha Rai,[†,⊥] Ajit Jadhav,[†] Lena Schultz,[†] Michelle Armstrong,[||] J. Brian Jameson, II,[||] Steven Perry,[||] Netra Joshi,[||] James M. Bougie,[†] William Leister,[†] David A. Taylor-Fishwick,[‡] Jerry L. Nadler,[‡] Michael Holinstat,[§] Anton Simeonov,[†] David J. Maloney,[*,†] and Theodore R. Holman[*,||]

[†]NIH Chemical Genomics Center, National Human Genome Research Institute, National Institutes of Health, 9800 Medical Center Drive, MSC 3370 Bethesda, Maryland 20892-3370, United States

[‡]Department of Internal Medicine, Strelitz Diabetes Center, Eastern Virginia Medical School, Norfolk, Virginia 23501-1980, United States

[§]Department of Medicine, Cardeza Foundation for Hematologic Research, Thomas Jefferson University, Philadelphia, Pennsylvania 19107, United States

[||]Department of Chemistry and Biochemistry, University of California, Santa Cruz, 250 Physical Sciences Building, Santa Cruz, California 95064, United States

Supporting Information

**ABSTRACT:** We report the discovery of novel small molecule inhibitors of platelet-type 12-human lipoxygenase, which display nanomolar activity against the purified enzyme, using a quantitative high-throughput screen (qHTS) on a library of 153607 compounds. These compounds also exhibit excellent specificity, >50-fold selectivity vs the paralogues, 5-human lipoxygenase, reticulocyte 15-human lipoxygenase type-1, and epithelial 15-human lipoxygenase type-2, and >100-fold selectivity vs ovine cyclooxygenase-1 and human cyclooxygenase-2. Kinetic experiments indicate this chemotype is a noncompetitive inhibitor that does not reduce the active site iron. Moreover, chiral HPLC separation of two of the racemic lead molecules revealed a strong preference for the (−)-enantiomers ($IC_{50}$ of 0.43 ± 0.04 and 0.38 ± 0.05 $\mu$M) compared to the (+)-enantiomers ($IC_{50}$ of >25 $\mu$M for both), indicating a fine degree of selectivity in the active site due to chiral geometry. In addition, these compounds demonstrate efficacy in cellular models, which underscores their relevance to disease modification.

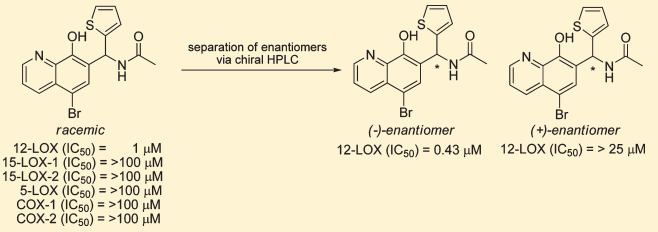


## INTRODUCTION

Lipoxygenases (LOXs) are nonheme, iron-containing enzymes that are ubiquitous in the plant and animal kingdoms. LOXs regio- and stereospecifically peroxidate polyunsaturated fatty acids (e.g., arachidonic acid (AA) and linoleic acid (LA)) containing *cis*,*cis*-1,4-pentadiene moieties to form the corresponding hydroperoxy fatty acids.[1] LOXs are the first committed step in a cascade of metabolic pathways that are implicated in the onset of inflammatory diseases such as cancers, heart disease, and asthmas,[2−5] making LOXs ideal candidates for pharmaceutical inhibitory treatment. However, the discovery of selective, potent inhibitors is critical to providing relevant chemical tools and probes to investigate LOXs involvement in inflammation and disease states.

Human LOXs are distributed among a variety of tissues and cellular locations and have been implicated in numerous disease states. 5-LOX shuttles between the cytosol and nuclear membrane[6,7] and has been implicated in cancer[8−10] and asthma.[5,7] Despite 5-LOX having been targeted by pharmaceutical companies for many years,[11] Zileutin, developed by the Abbott laboratories, remains the only FDA approved drug which targets a human lipoxygenase.[12] Both Pfizer and Merck have developed potent and selective inhibitors of 5-LOX (PF-4191834[13] and MK-0633,[14] respectively), however, both of these appear to have been discontinued from further clinical development.[15] Reticulocyte 15-LOX-1 has been implicated in colorectal[16,17] and prostate[18−21] cancers, while epithelial 15-LOX-2 is expressed in hair, prostate, lung, and cornea[22,23] and has been demonstrated to have an inverse correlation of expression and prostate cancer.[24,25] Mutations in epidermis-type lipoxygenase-3 and 12-(*R*)-LOX, which are expressed in the skin, have been shown to cause nonbullous congenital ichthyosiform erythroderma.[26] Human platelet-type 12-(*S*)-LOX (12-LOX), for which the current study focuses on, has been implicated in skin disease,[27] pancreatic,[28] breast,[29,30] prostate cancers,[21] diabetes,[31] and blood coagulation[32] and platelet activation.[33,34]

**Received:** April 26, 2011
**Published:** July 08, 2011

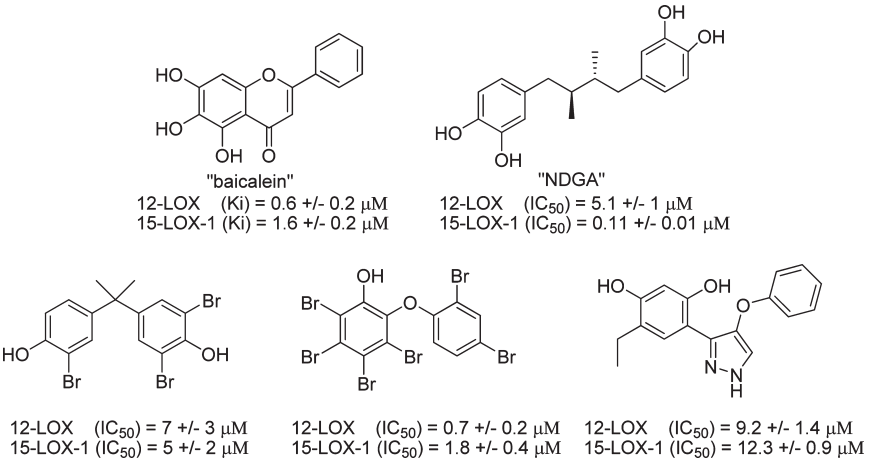


**Figure 1.** Previously reported 12-LOX inhibitors.

Previous studies have demonstrated elevated 12-LOX mRNA expression levels in cancerous prostate tissue cell lines[35] and that addition of 12-*S*-hydroxyeicosatetraenoic acid (12-HETE) to human prostate adenocarcinoma cells increased their motility and ability to invade neighboring tissues. This study has been supplemented with recent data that demonstrates 12-LOX enhances the excretion and expression of vascular endothelial growth factor (VEGF)[35] under hypoxic conditions by up-regulating the protein level, mRNA, and functionality of hypoxia inducible factor-1 alpha (HIF-1α), a transcription factor that up-regulates VEGF activity.[36] Taken together, these studies provide a case for the involvement of 12-LOX in prostate cancer. Additional reports have implicated 12-LOX in breast cancer. 12-LOX mRNA was found to have an increased expression in breast cancer tissue cell lines versus noncancerous breast epithelial cell lines, where the addition of the LOX inhibitor cinnamyl-3,4-dihydroxy-α-cyanocinnamate dramatically inhibited the growth of the breast cancer cell lines.[37] Increased expression of 12-LOX mRNA has also been witnessed in tissues extracted from patients with breast cancer[38−40] versus healthy adjacent tissue. 12-LOX is also expressed in human pancreatic islets, which increases with inflammatory cytokines and the 12-HETE generated leads to reduced insulin secretion and pancreatic $\beta$ cell damage.[31]

There have been many attempts to discover selective and potent 12-LOX inhibitors with limited success. Past drug discovery efforts for human lipoxygenases have utilized traditional medicinal chemistry[41−49] and natural product isolation,[50−58] yielding compounds that are reductive or promiscuous phenolic/terpene-based inhibitors. Other reports have focused on pharmacophore virtual screening[59] to yield novel, selective inhibitors for rabbit 15-LOX. However, there are few 12-LOX inhibitors that are selective or potent and even fewer which are both.[58,60−62]

Several natural products have been shown to exhibit micromolar inhibition of 12-LOX, particularly Hinokitiol[58] and the catechins from green tea leaf extract,[62] albeit with moderate selectivity over other human LOXs. Our laboratory has discovered and investigated many nonselective 12-LOX inhibitors. Investigations of marine derived natural products yielded brominated aryl phenols,[57] and an SAR study, with the known reductive LOX inhibitor, nordihydroguaiaretic acid (NDGA, a pan-lipoxygenase inhibitor), yielded a variety of potent derivatives as shown in Figure 1.[63] It should be noted that the mistakenly identified 12-LOX selective inhibitor, baicalein, was shown, through steady-state kinetics, to not be selective in vitro and in fact is equipotent against both 15-LOX-1 and 12-LOX.[64]

In an attempt to move from screening to more structure-based design, our laboratory recently identified several nonreductive inhibitors for 12-LOX and 15-LOX-1 by performing docking to homology models, however these compounds displayed weak potency and poor selectivity.[65] Our laboratory has also recently discovered four potent and selective 12-LOX inhibitors while testing a high-throughput screen (HTS) against the National Cancer Institute repository and the UC Santa Cruz Marine Extract Library.[60] Unfortunately, these compounds were not drug-like and not amenable to modification.

Because of the dearth of selective and potent 12-LOX inhibitors and the potential therapeutic benefit for such compounds, herein we have performed a quantitative HTS (qHTS) against a large library of 153607 small molecules[66] in conjunction with the NIH Molecular Libraries Probe Production Center Network (MLPCN) in search of novel, potent, and selective 12-LOX inhibitors. We report the discovery and SAR of an 8-hydroxyquinoline-based scaffold with nanomolar potency that is selective over the related human isoforms, 5-LOX, reticulocyte 15-LOX-1, epithelial 15-LOX-2, as well as ovine cyclooxygenase-1 and human cyclooxygenase-2. In addition, the mode of inhibition and the mechanism of action are discussed.

## CHEMISTRY

The synthesis of analogues (**1**−**30**: see Table 1) could be rapidly accomplished utilizing the Betti reaction (a type of Mannich reaction, Scheme 1).[67−69] After optimization of the reaction conditions, it was found that the reaction worked best in the absence of solvent (neat) and at temperatures between 120 and 160 °C (160 °C when $R_2$ = F, 150 °C when $R_2$ = Cl or $NO_2$, and 120 °C when $R_2$ = Br (with overnight heating). One of the initial challenges that had to be overcome was purification of these substrates. While ultimately these could be purified via standard reversed-phase prep-HPLC, we found them to be not well-behaved and often resulted in having to reprep the samples to achieve >95% purity. However, we found that recrystallization using ethanol or a mixture of ethanol−DMF provided the pure product without any chromatographic purification. This method allowed for the rapid preparation of a wide variety of analogues for SAR investigations. The synthesis of **31** and **33** (see Table 2)


dx.doi.org/10.1021/jm2005089 |*J. Med. Chem.* 2011, 54, 5485–5497

**Table 1. 12-LOX Inhibition of Analogues (1−30)[a]**

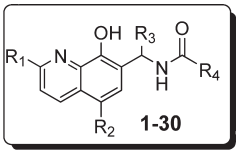


| compd | $R_1$ | $R_2$ | $R_3$ | $R_4$ | $IC_{50}$ ($\mu$M) [± SD ($\mu$M)] |
|---|---|---|---|---|---|
| **1** | H | $NO_2$ | thiophene | $CH_2CH_3$ | 0.8 [0.2] |
| **2** | H | Cl | thiophene | $CH_2CH_3$ | 1.0 [0.3] |
| **3** | H | Cl | thiophene | $CH_3$ | 1.0 [0.1] |
| **4** | H | Br | thiophene | $CH_2CH_3$ | 14 [3.0] |
| **5** | H | Br | thiophene | $CH_3$ | 1.0 [0.2] |
| **6** | H | H | thiophene | $CH_2CH3$ | 3.4 [0.6] |
| **7** | H | F | thiophene | $CH_3$ | 2.0 [0.2] |
| **8** | H | $NO_2$ | furan | $CH_2CH_3$ | 1.2 [0.4] |
| **9** | H | Cl | furan | $CH_2CH_3$ | 1.0 [0.2] |
| **10** | H | Cl | furan | $CH_3$ | 3.0 [0.5] |
| **11** | H | Br | furan | $CH_2CH_3$ | 2.0 [0.5] |
| **12** | H | Br | furan | $CH_3$ | 2.0 [0.3] |
| **13** | H | F | furan | $CH_3$ | 5.0 [1] |
| **14** | H | Cl | cyclopropane | $CH_2CH_3$ | 1.6 [0.3] |
| **15** | H | Cl | cyclopropane | $CH_3$ | 3.0 [0.6] |
| **16** | H | Cl | isopropyl | $CH_2CH_3$ | 1.2 [0.4] |
| **17** | H | Cl | isopropyl | $CH_3$ | 2.6 [0.4] |
| **18** | H | Cl | methyl | $CH_2CH_3$ | >50 |
| **19** | H | Cl | methyl | $CH_3$ | >150 |
| **20** | H | F | methyl | $CH_3$ | >75 |
| **21** | H | Cl | H | $CH_3$ | >150 |
| **22** | H | Cl | 5-Me-thiophene | $CH_2CH_3$ | 3.5 [1] |
| **23** | H | Cl | 5-bromofuran | $CH_2CH_3$ | >75 |
| **24** | Cl | Cl | furan | $CH_3$ | >75 |
| **25** | $N(Me)_2$ | Cl | furan | $CH_3$ | >75 |
| **26** | piperidine | Cl | furan | $CH_3$ | >75 |
| **27** | H | Cl | 4-Me-Ph | $CH_2CH_3$ | >150 |
| **28** | H | Cl | 4-F-Ph | $CH_2CH_3$ | >50 |
| **29** | H | Cl | furan | Ph | >25 |
| **30** | H | Cl | furan | 4-Me-Ph | >25 |

[a] The UV−vis-based manual inhibition data (3 replicates) were fit as described in the Methods section.

**Scheme 1. Synthesis of 8-Hydroxyquinoline Analogues (1−30)**

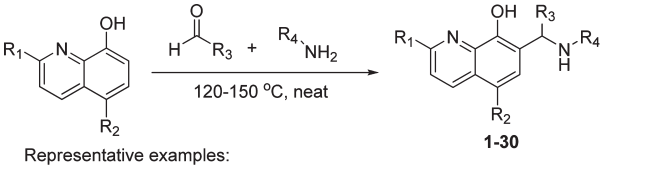


Representative examples:

$R_1$ = Cl, $N(Me)_2$, piperidine, H
$R_2$ = Cl, Br, F, $NO_2$, H
$R_3$ = thiophen-2-yl, furan-2-yl, cyclopropyl, methyl, isopropyl, phenyl, H
$R_4$ = $C(O)CH_3$, $C(O)CH_2CH_3$, C(O)Ph

were conveniently achieved utilizing a common intermediate **9**. Accordingly, treatment of analogue **9** with iodomethane and KOH gave the methoxy derivative **31** in good yield. Piperidine analogue **33** was synthesized via a Rh-catalyzed reduction of **9** under an atmosphere of hydrogen using methanol as a solvent. Naphthol derivatives, such as compound **32**, were synthesized in a similar manner as analogues **1**−**30**, except longer reaction time and lower temperatures were required for optimal yields (55 °C, 15 h, see Supporting Information for a detailed synthetic procedure for **31**−**33**).

**Table 2. 12-LOX Inhibition of Analogues (31−33)[a]**

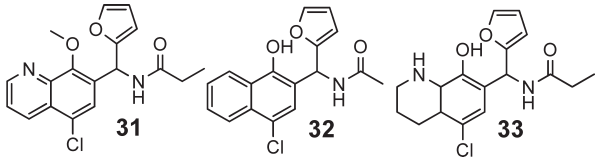


| compd | $IC_{50}$ ($\mu$M) [± SD ($\mu$M)] |
|---|---|
| **31** | >75 |
| **32** | >75 |
| **33** | 3.0 [0.7] |

[a] The UV−vis-based manual inhibition data were fit as described in the Methods section.

## RESULTS AND DISCUSSION

To discover novel inhibitors of 12-LOX, we utilized a chromogenic assay to detect the hydroperoxide lipoxygenase reaction products, as described elsewhere.[70] Briefly, after allowing the lipoxygenase reaction to proceed to the desired completion point, ferrous Xylenol Orange was added, and the purple product, generated by the oxidation of the ferrous ions to ferric ions by the hydroperoxide, was quantitated using visible light absorbance detection. Prior to the screen, the reaction parameters (concentrations of substrate and enzyme, percent substrate conversion, reagent stability under working conditions) were tested and optimized to ensure adequate performance (data not shown). The screen of the entire library involved testing each of the 153607 compounds as a dilution series of seven or more concentrations spanning the 57 $\mu$M to 0.7 nM range. This was accomplished by testing 936 assay plates in a fully automated robotic system (Methods). The screen was associated with a high signal-to-background average of 4.29 and an average $Z'$ factor of 0.69 (Supporting Information, Figure S1A). NDGA, present on every screening plate as a 16-point dose−response, exhibited consistent $IC_{50}$ throughout the screen.

Screening data analysis included classification of the concentration responses based on curve shape, presence of asymptotes, efficacy, and $IC_{50}$, as described elsewhere.[71] In addition to 149407 inactive samples and 2295 inconclusive responses, samples belonging to 67 clusters of structurally similar primary screening hits and 124 singletons were associated with complete concentration−response curves (Supporting Information, Figure S1B). Further prioritization based on potency and synthetic tractability led to selection of 59 compounds for additional testing. Complete screening and follow-up data have been made available in PubChem (PubChem BioAssay identifier 2164). Orthogonal confirmation of the hits from the qHTS, using a UV−vis-based manual assay, yielded an 8-hydroxyquinoline (8-HQ) based chemotype, compound **1** (Figure 2), that displayed micromolar to submicromolar potency, with an $IC_{50}$ of 0.8 ± 0.2 $\mu$M. To investigate


dx.doi.org/10.1021/jm2005089 |J. Med. Chem. 2011, 54, 5485–5497

requirements for inhibition and potency, we prepared derivatives of the 8-HQ scaffold that were chemically modified at the $R_1$, $R_2$, $R_3$, and $R_4$ positions (see Table 1). In general, the core scaffold of **1** was tolerant to a variety of changes in size and electrostatics in the $R_2$, $R_3$, and $R_4$ positions without dramatic changes in potency, however, there were several combinations of modifications that were not well tolerated.

Investigations of various substituents at $R_3$ revealed that compared to the thiophene or furan moiety, both smaller groups ($R_3$ = Me, entries **18**−**20** and $R_3$ = H, entry **21**) and larger groups ($R_3$ = 4-Me-Ph, entry **27** and $R_3$ = 4-F-Ph, entry **28**) resulted in essentially complete loss in activity. However, thiophene, furan, cyclopropyl, cyclopentyl, and isopropyl groups at this position all showed comparable activity.

While only limited investigation at $R_1$ was conducted, all modifications at this position led to loss in activity (entries **24**−**26**), suggesting that the binding pocket does not tolerate increased steric bulk in this position. Similarly, increasing the size of the substituents off the amide ($R_4$) was not beneficial for improved activity, as shown with analogues **29** and **30** (R = Ph and 4-Me-Ph, respectively). Additionally, $R_4$ = $CH(CH_3)_2$ and $(CH_2)_2CH_3$ were synthesized and these analogues also displayed weak potency (data not shown). In contrast, modifications to $R_2$ was well tolerated, with H, Cl, Br, F, $NO_2$ all showing comparable activity.

8-HQ scaffolds are known metal chelators,[72] and chelation of the LOX active site iron has been documented in the literature previously.[73,74] Consequently, we sought to investigate the chemical requirements for metal chelation by modifying the oxygen and nitrogen ligands that could bind the active site iron (Table 2, see compounds **31**−**33**). Both methylation of the phenol (entry **31**) and removal of the ring nitrogen (analogue **32**) resulted in a loss of potency. However, when the pyridine was reduced to the piperidine (analogue **33**), a nonrigid heterocycle, the inhibition was unaffected ($IC_{50}$ = 3.0 ± 0.7 μM). This data is consistent with the inhibitors ligating the metal in a bidentate fashion, given that piperidines are comparable in ligand strength to pyridine[75] and that neither of the monodentate modifications of the 8-HQ core inhibit 12-LOX. This hypothesis is supported by the fact that modifications at $R_1$ (**24**, **25**, **26**) also lower potency, presumably due to sterics as the 8-HQ moiety binds the iron. Other small molecule 8-HQs, such as 8-HQ-5-sulfonic acid and 8-HQ-5-nitro, were found to be weak inhibitors ($IC_{50}$ values >80 μM against 12-LOX), however, 5,7-dichloro-8-HQ (chloroxine) was an exception. It effectively inhibited all LOX isozymes tested ($IC_{50}$ values, 5-LOX = 3.6 ± 0.8 μM, 12-LOX = 1.9 ± 0.4 μM, 15-LOX-1 = 2.4 ± 0.4 μM, 15-LOX-2 = 28 ± 7 μM). Interestingly, chloroxine is a topical antimicrobial agent used in the treatment of seborrheic dermatitis, and while no studies have linked lipoxygenase to this ailment, inflammation has been implicated in its treatment, suggesting a possible connection.[76]

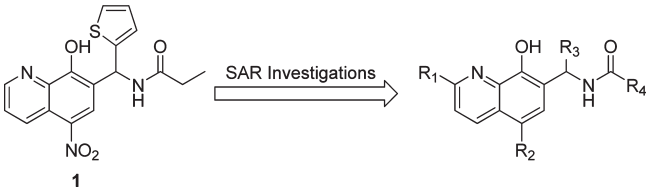


**Figure 2.** Lead compound (**1**) and positions explored for SAR.

We have attempted to characterize these inhibitors binding directly to the active site ferrous and ferric ion, using UV and fluorescence spectroscopy, however neither experiment was successful. 12-LOX loses activity dramatically as it concentrates, thus making it difficult to achieve enzyme concentrations that would yield a signal of sufficient intensity to observe.

Our final investigation into the SAR around the 8-HQ scaffold was to determine whether the two enantiomers had differential potency. As such, we utilized normal-phase chiral HPLC to effectively separate the enantiomers of both analogues **2** and **5** as shown in Table 3 (HPLC traces, Supporting Information, Figure S2 and S3). Both (−)-**2** (aka **36**) and (−)-**5** (aka **34**) displayed 12-LOX inhibition at approximately half the $IC_{50}$ value of the racemic mixture (**34** (−)-enantiomer, $IC_{50}$ = 0.43 ± 0.04 μM; (racemic)-**5**, $IC_{50}$ = 1.0 ± 0.2 μM; **36** (−)-enantiomer, $IC_{50}$ = 0.38 ± 0.05 μM; (racemic)-**2**, $IC_{50}$ = 1.0 ± 0.3 μM). In contrast, (+)-**2** (aka **37**) and (+)-**5** (aka **35**) displayed no inhibition ($IC_{50}$ > 25 μM), indicating a fine degree of selectivity in the active site due to chiral geometry. We are currently attempting to crystallize the active enantiomers to determine their absolute stereochemistry.

The above data is suggestive that these inhibitors bind directly to the active site iron, which raises the possibility that these inhibitors could have the necessary redox potential to reduce the active ferric iron to the resting ferrous state, as has been reported previously.[63,64,77,78] To investigate the redox potential of this chemotype, DPPH, a free radical scavenger, was incubated with compound **1** and no reduction of DPPH was observed. Stoichiometric reduction of DPPH was achieved by the known reductive LOX inhibitor, NDGA, suggesting that these 8-HQ inhibitors are

**Table 3. 12-LOX Inhibition of Enantiomerically Pure Analogues (34−37)**[a]

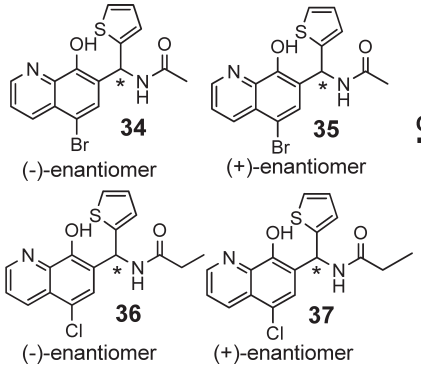


| Compound | $IC_{50}$ (μM) [+/- SD (μM)] |
|---|---|
| **34** | 0.43 [0.04] |
| **35** | >25 |
| **36** | 0.38 [0.05] |
| **37** | >25 |

[a] The UV−vis-based manual inhibition data were fit as described in the Methods section.


dx.doi.org/10.1021/jm2005089 |J. Med. Chem. 2011, 54, 5485–5497

not reductive in nature. Unfortunately, measuring the oxidation of the inhibitor (reduction of the active site iron) with the pseudoperoxidase assay is not possible with 12-LOX due to a lack of absorbance change at 234 nm. Another mechanism of inhibition seen for LOX is promiscuous inhibition due to small molecule aggregates.[79] Compound **3** was therefore screened with increasing amounts of Triton X-100, from 0.005% to 0.02%, with negligible changes in the $IC_{50}$, indicating that small molecule aggregates are not responsible for inhibition.

In addition to characterizing the inhibition constants, the mode of binding was investigated with steady state kinetics using compound **3** by monitoring the formation of 12-HPETE as a function of substrate and inhibitor concentration in the presence of 0.01% Triton-X-100. Replots of $K_M/k_{cat}$ and $1/k_{cat}$ versus inhibitor concentration (Supporting Information, Figure S4A,B) yielded linear plots, with $K_{ic}$ equaling 0.7 ± 0.09 $\mu$M and $K_{iu}$ equaling 0.8 ± 0.1 $\mu$M, which are defined as the equilibrium constants of dissociation from the enzyme and enzyme substrate complex, respectively. The similar affinity of inhibitor binding to both the enzyme and the enzyme substrate complex ($K_{ic}$ is approximately $K_{iu}$) is a rare example of true noncompetitive inhibition,[80] whose inhibitor affinity is not affected by substrate binding. Regarding the chemical mechanism of inhibition, compound **2** did not display a time-dependent inhibition when it was incubated with 12-LOX, unlike the time dependent inhibition seen for the bidentate catechol inhibitors against sLO-1[74] and the 8-HQ derivatives against macrophage migration inhibitory factor (MIF).[81] This data may suggest that compound **2** is not an irreversible inhibitor, however, this could not be proven due to the inactivation of 12-LOX upon dialysis.

To determine the selectivity of this inhibitor chemotype, a subset of compounds was screened against a variety of LOX isozymes (Table 4). In general, the selectivity was excellent, with the potency difference being 25- to 150-fold against 15-LOX-1, 45- to 1300-fold against 5-LOX, and 45- to 150-fold against 15-LOX-2. Chiral analogue, **36**, was not only the most potent of the inhibitors but it also had some of the best selectivity relative to 5-LOX (1300-fold) and 15-LOX-1 (130-fold). Interestingly, the selectivity of this chemotype between 12-LOX and 15-LOX-1 is less than that between 12-LOX and 5-LOX, which may be accounted for by the similar active sites of 12-LOX and 15-LOX-1.[82]

Compound **5** was also screened against the mouse 12/15-lipoxygenase (12/15-LOX), which generates predominately 12-HPETE, with a smaller percentage of 15-HPETE and it had an $IC_{50}$ value of 14 ± 3.0 $\mu$M. While this value is over 10-fold larger than that for 12-LOX, it is still significantly lower than the $IC_{50}$ of **5** against 15-LOX-1 ($IC_{50}$ >150 $\mu$M), suggesting the active site of 12/15-LOX is more similar to 12-LOX than 15-LOX-1. This was further supported when a highly specific inhibitor against 15-LOX-1 ($IC_{50}$ < 10 nM against 15-LOX-1) showed an $IC_{50}$ of greater than 75 $\mu$M against 12/15-LOX.[70] In addition, compound **5** did not inhibit either cyclooxygenase-1 (COX-1) or COX-2 ($IC_{50}$ > 100 $\mu$M for both), demonstrating a selectivity of greater than 100-fold for 12-LOX over both COX-1 and COX-2.

To demonstrate the potential for these compounds to be utilized in more advanced biological systems (e.g., cell-based assays), we investigated various in vitro ADME properties of a representative compound (analogue **34**) as shown in Table 5. This chemotype was found to have acceptable kinetic solubility. It should be noted that these conditions are different from the conditions used for the $IC_{50}$ determinations, which had detergent, lower salt concentrations, and higher pH, all leading to greater inhibitor solubility. The inhibitor also showed good cell permeability and excellent stability in PBS buffer and mouse plasma. However, the compound was susceptible to metabolism by mouse liver microsomes with a $T_{1/2}$ of under 10 min. Despite this result, we were eager to determine the in vivo PK of this molecule to provide a basis for future investigations in disease relevant mouse models. As shown in Table 6, compound **34** had a reasonable plasma $T_{1/2}$ of 3.5 h and a $C_{max}$ of 288 $\mu$M. Importantly, the exposure level exceeded the purified enzyme assay $IC_{50}$ for the full 24 h period and $IC_{50}$ in the platelet assay (vide infra) for 8 h. Moreover, this compound does not efficiently cross the blood−brain barrier (BBB), which for the treatment of diseases such as diabetes and thrombosis is considered a desirable result as CNS-active compounds could result in undesired side effects. These in vitro ADME and in vivo PK results suggest that the molecules described above should provide utility in probing the effects of 12-LOX inhibition in both cell-based assays and possibly in vivo models.

Other groups have postulated that 7-substituted-8-HQ derivatives, which contain substituted anilines in place of the amide moiety (at C-9), undergo a retro-Mannich reaction to afford a reactive species that can form a variety of covalent adducts (see Figure 3b).[83] In agreement with these findings, we too found such analogues (aniline as opposed to amide group at C-9) were relatively unstable in both assay buffer and mouse plasma. However, as shown above, our lead compounds are completely stable in both PBS buffer (pH 7.4) and mouse plasma over a 48 h period. Moreover, this particular chemotype displayed favorable exposure levels in vivo (mouse) as described above. These findings suggest that the retro-Mannich pathway is much less facile for the amide-containing series, potentially as a result of amide

**Table 4. Selectivity Profile of Representative Analogues**[a]

| | $IC_{50}$ ($\mu$M) | | | |
|---|---|---|---|---|
| compd | 12-LOX | 5-LOX | 15-LOX-1 | 15-LOX-2 |
| **1** | 0.8 | ND | >25 | ND |
| **3** | 1.0 | >100 | >25 | ND |
| **5** | 1.0 | >100 | >100 | >100 |
| **6** | 3.4 | >100 | >50 | >100 |
| **9** | 1.0 | >100 | >50 | >100 |
| **34** | 0.43 | >100 | >30 | ND |
| **36** | 0.38 | >100 | >50 | ND |

[a] The UV−vis-based manual inhibition data (3 replicates) were fit as described in the Methods section.

**Table 5. In Vitro ADME Properties for Representative Analogue (Compound 34)**[a]

| compd | aq kinetic soln (PBS @ pH 7.4) ($\mu$M) | Caco-2 ($P_{app}10^{-6}$ m/s @ pH 7.4) | efflux ratio (B→A)/(A→B) | mouse liver microsome stability ($T_{1/2}$) (min) | PBS-pH7.4 stability: % remaining after 48 h | mouse plasma stability: % remaining after 48 h |
|---|---|---|---|---|---|---|
| **34** | 14.5 | 8.8 | 2.3 | <10 | 100 | 98.3 |

[a] Kinetic solubility measurements were conducted at Analiza Inc. using nitrogen detection methodologies. Caco-2 permeability, microsomal stability, and mouse plasma stability experiments were conducted at Pharmaron Inc.


dx.doi.org/10.1021/jm2005089 |J. Med. Chem. 2011, 54, 5485–5497

**Table 6. In Vivo PK Data for Representative Analogue (Compound 34)**[a]

| compd | $t_{1/2}$ (h) [plasma] | $t_{1/2}$ (h) [brain] | [brain/plasma] [b] | $C_{max}$ ($\mu$M) [plasma] | $C_{max}$ ($\mu$M) [brain] | $t_{max}$ (h) [plasma] | $t_{max}$ (h) [brain] | cLogP |
|---|---|---|---|---|---|---|---|---|
| **34** | 3.5 | 1.7 | 0.01 | 288 | 5 | 0.25 | 0.5 | 2.8 |

[a] Intraperitoneal (IP) administration (30 mg/kg body weight (mpk)), CD1 mice, $n$ = 3, monitored at 8 time points (0.25, 0.5, 1, 2, 4, 8, 12, 24 h). Compound **34** formulated as a suspension in 50% PEG 200 and 10% Cremophor EL in saline solution. [b] Calculated based on the average $[b/p]$ ratio over 8 time points (24 h period). Experiments were performed by Pharmaron Inc.

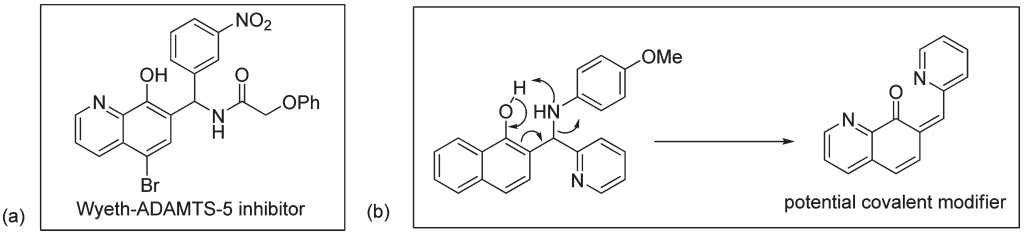


**Figure 3.** (a) Representative 8-HQ-based ADAMTS-5 inhibitor reported by Wyeth researchers with amide nitrogen at C-9. (b) Proposed mechanism of covalent modification for 8-HQs with aniline nitrogen at C-9.

nitrogen being less basic than the corresponding aniline nitrogen. A comparable 8-HQ chemical series was reported by Wyeth researchers as ADAMTS inhibitors, which like our chemotype contains the amide moiety at C-9 (Figure 3a). They found that the compound displayed good ADME properties (CYP inhibition and microsomal stability), supporting the notion that this subtle structural difference may have a drastic effect on the overall stability of this class of compounds.[84]

A select group of inhibitors, **1**, **34**, and **35**, were then tested for efficacy in a platelet cellular assay. Human platelets are known to express large amounts of 12-LOX upon stimulation of the protease-activated receptor (PAR) with its activating peptide, PAR1-AP.[33] We therefore incubated our inhibitors with human platelets, followed by stimulation with PAR1-AP and measured the change in 12-HETE production. In three separate experiments, 100 $\mu$M of **1** and **34** showed significant inhibition of PAR1-AP-mediated 12-HETE production, while **35** showed no reduction in 12-HETE production. This data confirms the in vitro data, where both **1** and **34** are potent ($IC_{50}$ values of 0.8 and 0.43 $\mu$M, respectively), while **35** is inactive ($IC_{50}$ value >25 $\mu$M) and supports the notion that the potent in vitro inhibitors inhibit 12-LOX intracellularly. A more thorough titration of inhibition in the platelet cells was then performed with compounds **1** and **34** (inhibitor concentration ranging from 1 to 100 $\mu$M). The $IC_{50}$ values were determined to be 15 $\pm$ 10 for **1** and 13 $\pm$ 7 for **34** (Figure 4). These cell-based $IC_{50}$ values are over 25-fold greater than the isolated enzyme $IC_{50}$ values, which could be a result of limited solubility and/or intracellular metabolism of the inhibitors. We are currently testing various modifications of the inhibitor scaffold to improve the cellular potency with the hopes of applying these inhibitors as anticoagulation therapeutics.

The ability of compound **1** to inhibit the activity of 12-LOX in a diabetic disease relevant model was also assessed using primary human islets obtained from donated tissues. Upon stimulation with arachidonic acid and calcium ionophore, production of 12-HETE in donor islets is significantly increased (Figure 5). This increase was a consistent response across all donor islets tested, and the degree of response was compatible with donor variation. Inclusion of compound **1** at an assay concentration of 10 $\mu$M resulted in an uniform inhibition of 68.9 $\pm$ 14.5% across the three

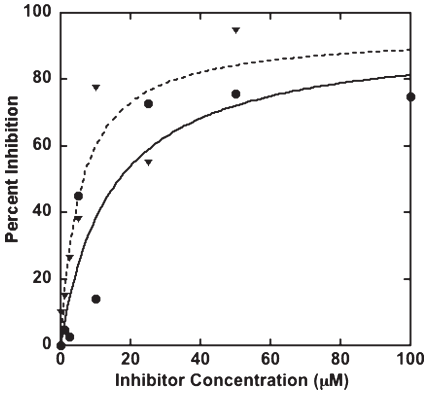


**Figure 4.** Titration curves of **1** (circles, solid line) and **34** (triangles, dashed line), against platelets, measuring inhibition of 12-HETE concentration by LC-MS-MS. Fitting the data to a simple hyperbolic curve yielded $IC_{50}$ values of 15 $\pm$ 10 $\mu$M for **1** and 13 $\pm$ 7 $\mu$M for **34**.

nondiabetic donors tested (Figure 5A). The basal and stimulated level of 12-HETE was elevated in islets from confirmed type 2 diabetic donors (Figure 5B). This is consistent with the relevance of 12-LOX to diabetes disease progression. Again, compound **1** resulted in an equivalent inhibition of stimulated 12-HETE production, 70 and 74%, respectively, in the two diabetic donors assayed.

## CONCLUSION

Because of the absence of selective, drug-like inhibitors of 12-LOX in the literature, a HTS campaign of 153607 compounds was performed that identified an 8-HQ chemotype as a novel, potent, and selective inhibitor of 12-LOX. Modifications to various positions around the core scaffold led to the development of an SAR profile. In general, the dynamic interplay between the various substitutions is not well understood, and while the SAR was relatively flat, several changes are not at all tolerated. The most dramatic loss of inhibition was observed at the C-2 position of the 8-HQ core ($R_1$), where all substitutions resulted in a complete loss of activity. Moreover, loss of activity was observed by removal of the nitrogen on the pyridine and/or methylation of


dx.doi.org/10.1021/jm2005089 |J. Med. Chem. 2011, 54, 5485–5497

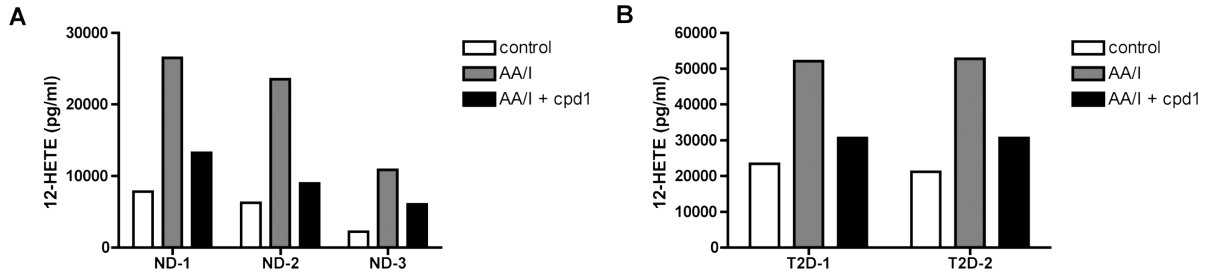


**Figure 5.** Inhibition of 12-HETE production in human donor islets. (A) 12-HETE levels form three nondiabetic donors (ND-1 to ND-3) either unstimulated (white bars) or stimulated for 60 min with 100 $\mu$M arachidonic acid (AA) and 30 min with 5 $\mu$M A23187 (I) in the absence (gray bars) or presence of 10 $\mu$M compound **1** (black bars). (B) shows 12-HETE levels in human islets from two confirmed type 2 diabetic donors (T2D-1 and T2D-2). Conditions are as described in (A).

the 8-hydroxy group, which strongly suggests the inhibitor is binding to the catalytic iron in a bidentate fashion. Further investigations demonstrated the (−)-enantiomers of this 8-HQ chemotype are seemingly responsible for the observed activity, with $IC_{50}$ values approximately half of the racemic mixture ($IC_{50}$ of 0.43 ± 0.04 for **34** and 0.38 ± 0.05 $\mu$M for **36**). 5-LOX, 15-LOX-1, 15-LOX-2, COX-1, and COX-2 were not inhibited by this chemotype. Interestingly, this chemotype did show weak inhibition against the 12/15-LOX ($IC_{50}$ = 14 $\mu$M), suggesting the active site of 12/15-LOX is more similar to 12-LOX than 15-LOX-1 (15-LOX-1 $IC_{50}$ > 150 $\mu$M). This is consistent with the fact that 15-LOX-1 selective inhibitors were inactive against 12/15-LOX and indicates caution when performing lipoxygenase studies on particular diseases with mouse models. Investigating the mode of inhibition demonstrated that this class of compounds is thought to be nonreductive and exhibits noncompetitive inhibition. We are currently investigating these compounds in cell-based diabetes and blood coagulation models, and it is our hope that this class of inhibitors will provide a molecular tool to determine the biological role of 12-LOX and further validate 12-LOX as a therapeutic target.

## EXPERIMENTAL SECTION

**General Chemistry.** Unless otherwise stated, all reactions were carried out under an atmosphere of dry argon or nitrogen in dried glassware. Indicated reaction temperatures refer to those of the reaction bath, while room temperature (rt) is noted as 25 °C. All solvents were of anhydrous quality purchased from Aldrich Chemical Co. and used as received. Commercially available starting materials and reagents were purchased from Aldrich and were used as received.

Analytical thin layer chromatography (TLC) was performed with Sigma Aldrich TLC plates (5 cm × 20 cm, 60 Å, 250 $\mu$m). Visualization was accomplished by irradiation under a 254 nm UV lamp. Chromatography on silica gel was performed using forced flow (liquid) of the indicated solvent system on Biotage KP-Sil prepacked cartridges and using the Biotage SP-1 automated chromatography system. $^1$H and $^{13}$C NMR spectra were recorded on a Varian Inova 400 MHz spectrometer. Chemical shifts are reported in ppm with the solvent resonance as the internal standard ($CDCl_3$ 7.26 ppm, 77.00 ppm, DMSO-$d_6$ 2.49 ppm, 39.51 ppm for $^1$H, $^{13}$C, respectively). Data are reported as follows: chemical shift, multiplicity (s = singlet, d = doublet, t = triplet, q = quartet, brs = broad singlet, m = multiplet), coupling constants, and number of protons. Low resolution mass spectra (electrospray ionization) were acquired on an Agilent Technologies 6130 quadrupole spectrometer coupled to the HPLC system. High resolution mass spectral data was collected in-house using an Agilent 6210 time-of-flight mass spectrometer, also coupled to an Agilent Technologies 1200 series HPLC system. If needed, products were purified via a Waters semipreparative HPLC equipped with a Phenomenex Luna C18 reverse phase (5 $\mu$m, 30 mm × 75 mm) column having a flow rate of 45 mL/min. The mobile phase was a mixture of acetonitrile (0.1% TFA) and $H_2O$ (0.1% TFA) at room temperature.

Samples were analyzed for purity on an Agilent 1200 series LC/MS equipped with a Luna C18 reverse phase (3 $\mu$m, 3 mm × 75 mm) column having a flow rate of 0.8−1.0 mL/min over a 7 min gradient and a 8.5 min run time. The mobile phase was a mixture of acetonitrile (0.025% TFA) and $H_2O$ (0.05% TFA), and the temperature was maintained at 50 °C. Purity of final compounds was determined to be >95%, using a 3 $\mu$L injection with quantitation by AUC at 220 and 254 nm (Agilent diode array detector).

**Chiral HPLC Separation of the Enantiomers.** Methanol was added to the sample until the sample was completely dissolved. Sample dissolution and analysis was performed at room temperature. The analytical analysis was performed on a Chiralcel OD column (4.6 mm × 150 mm, 5 $\mu$m). The mobile phase was 100% methanol at 1.0 mL/min. The sample was detected with a diode array detector (DAD) at 254 and 330 nm. Optical rotation (±) was determined with an in-line polarimeter (PDR-Chiral). Preparative purification was performed on a Chiralcel OD column (2 cm × 25 cm, 5 $\mu$m). The mobile phase was 100% methanol at 4.5 mL/min. Fraction collection was triggered by UV absorbance (330 nm). The LC system was limited to 100 $\mu$L injections. The fractions containing the requisite enantiomers were combined and concentrated under reduced pressure. The enantiomeric purity was determined by reinjection on the analytical column described above. The enantiomeric ratios (er) for all separated chiral compounds were found to be greater than 99:1. The optical rotations of the final compounds were obtained using a PerkinElmer model 341 polarimeter.

**General Procedure for the Synthesis of 8-HQ Analogues (Scheme 1).** Differentially substituted-quinolin-8-ol (1 equiv), amide (1.05 equiv), and the requisite aldehyde (1.1 equiv) were stirred neat at 120−160 °C for 15 min to 12 h (depending on the substituent at C-5). Upon heating, the reaction mixture melted and solid was formed after completion of the reaction. The solid product was washed with ethyl acetate, and the crude product was purified by recrystallization from ethanol or an ethanol−DMF mixture.

**Representative Characterization Data.** *N-((8-Hydroxy-5-nitroquinolin-7-yl)(thiophen-2-yl)methyl)propionamide (**1**).* LC-MS: rt (min) = 5.16. $^1$H NMR (DMSO-$d_6$) $\delta$ 1.03 (t, $J$ = 7.5 Hz, 3 H), 2.23 (qd, $J$ = 7.6 and 3.1 Hz, 2 H), 6.81 (dt, $J$ = 3.5 and 1.2 Hz, 1 H), 6.89 (dd, $J$ = 8.6 and 1.0 Hz, 1 H), 6.95 (dd, $J$ = 5.1 and 3.5 Hz, 1 H), 7.43 (dd, $J$ = 5.1 and 1.2 Hz, 1 H), 7.90 (dd, $J$ = 8.8 and 4.3 Hz, 1 H), 8.76 (s, 1 H), 9.02 (dd, $J$ = 4.1 and 1.6 Hz, 1 H), 9.09 (d, $J$ = 8.8 Hz, 1 H), and 9.19 (dd, $J$ = 8.8 and 1.6 Hz, 1 H). $^{13}$C NMR (DMSO-$d_6$) $\delta$ 9.86, 28.38, 45.33, 121.73, 123.84, 125.21, 125.29, 125.35, 126.87, 127.23, 133.05, 134.37, 136.80, 145.17, 149.03, 157.34 and 172.29. HRMS ($m/z$): $[M + H]^+$ calcd for $C_{17}H_{16}N_3O_4S$, 358.0856; found, 358.0861.


dx.doi.org/10.1021/jm2005089 |J. Med. Chem. 2011, 54, 5485–5497

*N-((5-Chloro-8-hydroxyquinolin-7-yl)(thiophen-2-yl)methyl)propionamide (**2**).* LC-MS: rt (min) = 5.6. $^1$H NMR (DMSO-$d_6$) $\delta$ 1.03 (t, $J$ = 7.6 Hz, 3 H), 2.16−2.28 (m, 2 H), 6.75−6.78 (m, 1 H), 6.89−6.96 (m, 2 H), 7.40 (dd, $J$ = 5.1 and 1.0 Hz, 1 H), 7.74 (dd, $J$ = 8.6 and 4.1 Hz, 1 H), 7.79 (s, 1 H), 8.50 (dd, $J$ = 8.5 and 1.5 Hz, 1 H), 8.91 (d, $J$ = 8.8 Hz, 1 H), 8.98 (dd, $J$ = 4.1 and 1.4 Hz, 1 H) and 10.42 (brs, 1 H).; HRMS ($m/z$): $[M + H]^+$ calcd for $C_{17}H_{16}ClN_2O_2S$, 347.0618; found, 347.0621. (−)-**2** (e.g., **36**) $[\alpha]_D^{23} = -24$ ($c$ = 0.6, $CHCl_3$); (+)-**2** (e.g., **37**) $[\alpha]_D^{23} = +24$ ($c$ = 0.6, $CHCl_3$).

*N-((5-Chloro-8-hydroxyquinolin-7-yl)(thiophen-2-yl)methyl)acetamide (**3**).* LC-MS: rt (min) = 5.28. $^1$H NMR (DMSO-$d_6$) $\delta$ 1.94 (s, 3 H), 6.78 (d, $J$ = 3.5 Hz, 1 H), 6.89 (d, $J$ = 8.8 Hz, 1 H), 6.94 (dd, $J$ = 5.1 and 3.5 Hz, 1 H), 7.41 (dd, $J$ = 5.1 and 1.0 Hz, 1 H), 7.75 (dd, $J$ = 8.5 and 4.2 Hz, 1 H), 7.78 (s, 1 H), 8.51 (dd, $J$ = 8.6 and 1.4 Hz, 1 H), 8.96−9.02 (m, 2 H) and 10.43 (brs, 1 H)). HRMS ($m/z$): $[M + H]^+$ calcd for $C_{16}H_{14}ClN_2O_2S$, 333.0459; found, 333.0460.

*N-((5-Bromo-8-hydroxyquinolin-7-yl)(thiophen-2-yl)methyl)propionamide (**4**).* LC-MS: rt (min) = 5.70. $^1$H NMR (DMSO-$d_6$) $\delta$ 1.03 (t, $J$ = 7.5 Hz, 3 H), 2.16−2.29 (m, 2 H), 6.76 (d, $J$ = 3.3 Hz, 1 H), 6.87−6.96 (m, 2 H), 7.40 (dd, $J$ = 5.1 and 1.0 Hz, 1 H), 7.74 (dd, $J$ = 8.5 and 4.2 Hz, 1 H), 7.96 (s, 1 H), 8.43 (dd, $J$ = 8.6 and 1.4 Hz, 1 H), 8.86−8.99 (m, 2 H) and 10.45 (brs, 1 H). HRMS ($m/z$): $[M + H]^+$ calcd for $C_{17}H_{16}BrN_2O_2S$, 391.0105; found, 391.0108.

*N-((5-Bromo-8-hydroxyquinolin-7-yl)(thiophen-2-yl)methyl)acetamide (**5**) ML127.* LC-MS: rt (min) = 5.36. $^1$H NMR (DMSO-$d_6$) $\delta$ 1.94 (s, 3 H), 6.78 (dt, $J$ = 3.5 and 1.2 Hz, 1 H), 6.89 (dd, $J$ = 8.9 and 1.1 Hz, 1 H), 6.93 (dd, $J$ = 5.1 and 3.3 Hz, 1 H), 7.40 (dd, $J$ = 5.1 and 1.4 Hz, 1 H), 7.74 (dd, $J$ = 8.6 and 4.1 Hz, 1 H), 7.95 (s, 1 H), 8.43 (dd, $J$ = 8.5 Hz and 1.5 Hz, 1 H), 8.95 (dd, $J$ = 4.1 and 1.6 Hz, 1 H), 9.00 (d, $J$ = 8.8 Hz, 1 H) and 10.46 (brs, 1 H). $^{13}$C NMR (DMSO-$d_6$) $\delta$ 22.55, 45.35, 108.50, 123.41, 124.84, 125.08, 125.68, 126.34, 126.78, 129.38, 134.97, 138.89, 145.91, 149.24, 149.71, and 168.39. HRMS ($m/z$): $[M + H]^+$ calcd for $C_{16}H_{14}BrN_2O_2S$, 376.9954; found, 376.9956. (−)-**5** (e.g., **34**) $[\alpha]_D^{23} = -18$ ($c$ = 0.3, $CHCl_3$); (+)-**5** (e.g., **35**) $[\alpha]_D^{23} = +18$ ($c$ = 0.3, $CHCl_3$)

*N-((5-Fluoro-8-hydroxyquinolin-7-yl)(thiophen-2-yl)methyl)acetamide (**7**).* LC-MS: rt (min) = 4.76. $^1$H NMR (DMSO-$d_6$) $\delta$ 1.93 (s, 3 H), 6.77 (dt, $J$ = 3.5 and 1.2 Hz, 1 H), 6.88−6.95 (m, 2 H), 7.40 (dd, $J$ = 5.0 and 1.3 Hz, 1 H), 7.47 (d, $J$ = 11.2 Hz, 1 H), 7.68 (dd, $J$ = 8.5 and 4.2 Hz, 1 H), 8.44 (dd, $J$ = 8.5 and 1.7 Hz, 1 H), 8.91−8.99 (m, 2 H) and 10.07 (brs, 1 H). $^{13}$C NMR (DMSO-$d_6$) $\delta$ 22.55, 45.49, 104.54, 109.27, 109.48, 117.53, 117.72, 122.27, 123.67, 123.73, 124.86, 125.04, 126.73, 129.13, 129.16, 137.80, 137.83, 145.91, 146.04, 146.08, 148.17, 149.52, 150.60 and 168.37. HRMS ($m/z$): $[M + H]^+$ calcd for $C_{16}H_{14}FN_2O_2S$, 317.076; found, 317.0761.

*N-(Furan-2-yl(8-hydroxy-5-nitroquinolin-7-yl)methyl)propionamide (**8**).* LC-MS: rt (min) = 4.96. $^1$H NMR (DMSO-$d_6$) $\delta$ 1.01 (t, $J$ = 7.6 Hz, 3 H), 2.16−2.27 (m, 2 H), 6.13 (d, $J$ = 3.3 Hz, 1 H), 6.38 (dd, $J$ = 3.1 and 1.8 Hz, 1 H), 6.69 (d, $J$ = 8.4 Hz, 1 H), 7.61 (d, $J$ = 1.0 Hz, 1 H), 7.90 (dd, $J$ = 8.9 and 4.2 Hz, 1 H), 8.68 (s, 1 H), 8.97 (d, $J$ = 8.4 Hz, 1 H), 9.01 (dd, $J$ = 4.1 and 1.4 Hz, 1 H) and 9.17−9.21 (m, 1 H). HRMS ($m/z$): $[M + H]^+$ calcd for $C_{17}H_{16}N_3O_5$, 342.1084; found, 342.1082.

*N-((5-Chloro-8-hydroxyquinolin-7-yl)(furan-2-yl)methyl)propionamide (**9**).* LC-MS: rt (min) = 5.26. $^1$H NMR (DMSO-$d_6$) $\delta$ 1.01 (t, $J$ = 7.5 Hz, 3 H) 2.20 (qd, $J$ = 7.5 and 2.6 Hz, 2 H) 6.07 (d, $J$ = 3.1 Hz, 1 H) 6.37 (dd, $J$ = 3.0 and 1.9 Hz, 1 H) 6.72 (d, $J$ = 8.6 Hz, 1 H) 7.59 (s, 1 H) 7.66 - 7.89 (m, 2 H) 8.49 (dd, $J$ = 8.5 and 1.5 Hz, 1 H) 8.80 (d, $J$ = 8.8 Hz, 1 H) 8.97 (dd, $J$ = 4.2 and 1.5 Hz, 1 H) and 10.38 (brs, 1 H). $^{13}$C NMR (DMSO-$d_6$) $\delta$ 9.81, 28.28, 43.99, 106.95, 110.39, 118.47, 123.04, 123.07, 125.04, 126.15, 132.50, 138.62, 142.51, 149.16, 149.42, 153.95, and 172.21. HRMS ($m/z$): $[M + H]^+$ calcd for $C_{17}H_{16}ClN_2O_3$, 331.0844; found, 331.0849.

*N-((5-Chloro-8-hydroxyquinolin-7-yl)(furan-2-yl)methyl)acetamide (**10**).* LC-MS: rt (min) = 4.83. $^1$H NMR (DMSO-$d_6$) $\delta$ 1.92 (s, 3 H), 6.06−6.09 (m, 1 H), 6.37 (dd, $J$ = 3.2 and 1.9 Hz, 1 H), 6.70 (d, $J$ = 8.4 Hz, 1 H), 7.59 (dd, $J$ = 1.9 and 1.0 Hz, 1 H), 7.71 (s, 1 H), 7.74 (dd, $J$ = 8.5 and 4.2 Hz, 1 H), 8.50 (dd, $J$ = 8.6 and 1.6 Hz, 1 H), 8.88 (d, $J$ = 8.6 Hz, 1 H), 8.97 (dd, $J$ = 4.1 and 1.6 Hz, 1 H) and 10.39 (brs, 1 H). $^{13}$C NMR (DMSO-$d_6$) $\delta$ 22.51, 44.05, 106.99, 110.39, 118.48, 123.00, 123.05, 125.05, 126.14, 132.52, 138.62, 142.52, 149.19, 149.40, 153.86 and 168.47. HRMS ($m/z$): $[M + H]^+$ calcd for $C_{16}H_{14}ClN_2O_3$, 317.0687; found, 317.0689.

*N-((5-Bromo-8-hydroxyquinolin-7-yl)(furan-2-yl)methyl)propionamide (**11**).* LC-MS: rt (min) = 5.39. $^1$H NMR (DMSO-$d_6$) $\delta$ 1.01 (t, $J$ = 7.6 Hz, 3 H), 2.20 (qd, $J$ = 7.5 and 2.2 Hz, 2 H), 6.07 (d, $J$ = 3.1 Hz, 1 H), 6.37 (dd, $J$ = 3.2 and 1.9 Hz, 1 H), 6.71 (d, $J$ = 8.4 Hz, 1 H), 7.59 (dd, $J$ = 1.8 and 0.8 Hz, 1 H), 7.73 (dd, $J$ = 8.6 and 4.1 Hz, 1 H), 7.88 (s, 1 H), 8.42 (dd, $J$ = 8.6 and 1.6 Hz, 1 H), 8.81 (d, $J$ = 8.8 Hz, 1 H), 8.94 (dd, $J$ = 4.1 and 1.6 Hz, 1 H) and 10.41 (brs, 1 H). $^{13}$C NMR (DMSO-$d_6$) $\delta$ 9.81, 28.29, 43.96, 106.94, 108.33, 110.39, 123.38, 123.73, 126.35, 129.63, 134.95, 138.86, 142.51, 149.17, 150.03, 153.96, and 172.22. HRMS ($m/z$): $[M + H]^+$ calcd for $C_{17}H_{16}BrN_2O_3$, 375.0339; found, 375.0344.

*N-((5-Bromo-8-hydroxyquinolin-7-yl)(furan-2-yl)methyl)acetamide (**12**).* LC-MS: rt (min) = 5.03. $^1$H NMR (DMSO-$d_6$) $\delta$ 1.92 (s, 3 H), 6.04 - 6.11 (m, 1 H), 6.37 (dd, $J$ = 3.2 and 1.9 Hz, 1 H), 6.70 (d, $J$ = 8.6 Hz, 1 H), 7.56−7.62 (m, 1 H), 7.73 (dd, $J$ = 8.5 and 4.2 Hz, 1 H), 7.87 (s, 1 H), 8.43 (dd, $J$ = 8.6 and 1.6 Hz, 1 H), 8.89 (d, $J$ = 8.6 Hz, 1 H), 8.94 (dd, $J$ = 4.1 and 1.6 Hz, 1 H) and 10.42 (brs, 1 H). $^{13}$C NMR (DMSO-$d_6$) $\delta$ 22.51, 43.99, 106.96, 108.33, 110.39, 123.38, 123.65, 126.35, 129.61, 134.96, 138.86, 142.52, 149.18, 150.00, 153.87, and 168.47. HRMS ($m/z$): $[M + H]^+$ calcd for $C_{16}H_{14}BrN_2O_3$, 361.0182; found, 361.019.

**Methods.** *Biological Reagents.* All commercial fatty acids (Sigma-Aldrich Chemical Co.) were repurified using a Higgins HAIsil Semi-Preparative (5 $\mu$m, 250 mm × 10 mm) C-18 column. Solution A was 99.9% MeOH and 0.1% acetic acid; solution B was 99.9% $H_2O$ and 0.1% acetic acid. An isocratic elution of 85% A:15% B was used to purify all fatty acids, which were stored at −80 °C for a maximum of 6 months.

*Overexpression and Purification of Human 5-Lipoxygenase, Human 12-Lipoxygenase, and the Human 15-Lipoxygenases.* Human platelet 12-lipoxygenase (12-LOX), human reticulocyte 15-lipoxygenase-1 (15-LOX-1), human epithelial 15-lipoxygenase-2 (15-LOX-2), were expressed as N-terminally, $His_6$-tagged proteins and purified to greater than 90% purity, as evaluated by SDS-PAGE analysis.[50,85,86] Human 5-lipoxygenase was expressed as a nontagged protein and used as a crude ammonium sulfate protein fraction, as published previously.[87] Iron content of 12-LOX was determined with a Finnegan inductively coupled plasma mass spectrometer (ICP-MS), using cobalt-EDTA as an internal standard. Iron concentrations were compared to standardized iron solutions and used to normalize enzyme concentrations.

*High-Throughput Screen: Materials.* Dimethyl sulfoxide (DMSO) ACS grade was from Fisher, while ferrous ammonium sulfate, Xylenol Orange (XO), sulfuric acid, and Triton X-100 were obtained from Sigma-Aldrich.

*Compound Library.* A 153607 compound library was screened in 7−15 concentrations ranging from 0.7 nM to 57 $\mu$M. The library included 139798 diverse small drug-like molecules that are part of the NIH Small Molecule Repository. A collection of 2893 compounds from the Centers of Methodology and Library Development at Boston University (BUCMLD) and University of Pittsburgh (UPCMLD) were added to the library. Several combinatorial libraries from Pharmacopeia, Inc. totaled 1649 compounds. An additional 1981 compounds from the NCI Diversity Set were included. Last, 7286 compounds with known pharmacological activity were added to provide a large and diverse screening collection.

*High-Throughput Screening Protocol and HTS Analysis.* All screening operations were performed on a fully integrated robotic system (Kalypsys Inc., San Diego, CA) as described elsewhere.[88] First, 3 $\mu$L of enzyme (approximately 80 nM 12-LOX, final concentration) was dispensed into 1536-well Greiner black clear-bottom assay plate. Then compounds and controls (23 nL) were transferred via Kalypsys PinTool equipped with 1536-pin array. The plate was incubated for 15 min at room temperature, and then a 1 $\mu$L aliquot of substrate solution (50 $\mu$M

arachidonic acid final concentration) was added to start the reaction. The reaction was stopped after 6.5 min by the addition of 4 $\mu$L of FeXO solution (final concentrations of 200 $\mu$M Xylenol Orange (XO) and 300 $\mu$M ferrous ammonium sulfate in 50 mM sulfuric acid). After a short spin (1000 rpm, 15 s), the assay plate was incubated at room temperature for 30 min. The absorbances at 405 and 573 nm were recorded using ViewLux high-throughput CCD imager (Perkin-Elmer, Waltham, MA) using standard absorbance protocol settings. During dispensing, enzyme and substrate bottles were kept submerged into +4 °C recirculating chiller bath to minimize degradation. Plates containing DMSO only (instead of compound solutions) were included approximately every 50 plates throughout the screen to monitor any systematic trend in the assay signal associated with reagent dispenser variation or decrease in enzyme specific activity.

Data were analyzed in a similar method as described elsewhere.[71] Briefly, assay plate-based raw data were normalized to controls and plate-based data corrections were applied to filter out background noise. All concentration response curves (CRCs) were fitted using in-house developed software (http://ncgc.nih.gov/pub/openhts/). Curves were categorized into four classes: complete response curves (class 1), partial curves (class 2), single point actives (class 3), and inactives (class 4). Compounds with the highest quality, class 1 and class 2 curves, were prioritized for follow-up.

*Lipoxygenase UV−Vis-Based Manual Assay.* The initial one-point inhibition percentages were determined by following the formation of the conjugated diene product at 234 nm ($\varepsilon$ = 25000 $M^{-1}cm^{-1}$) with a Perkin-Elmer Lambda 40 UV/vis spectrophotometer at one inhibitor concentration. All reactions were 2 mL in volume and constantly stirred using a magnetic stir bar at room temperature (23 °C) with approximately 40 nM for 12-LOX (by iron content), 20 nM of 15-LOX-1 (by iron content), and 1 $\mu$M for 15-LOX-2 (by Bradford). Reactions with 12-LOX were carried out in 25 mM HEPES (pH 8.0) 0.01% Triton X-100 and 10 $\mu$M AA. Reactions with the crude, ammonium sulfate precipitated 5-LOX were carried out in 25 mM HEPES (pH 7.3), 0.3 mM $CaCl_2$, 0.1 mM EDTA, 0.2 mM ATP, 0.01% Triton X-100, and 10 $\mu$M AA. Reactions with 15-LOX-1 and 15-LOX-2 were carried out in 25 mM HEPES buffer (pH 7.5), 0.01% Triton X-100, and 10 $\mu$M AA. The concentration of AA (for 5-LOX, 12-LOX, and 15-LOX-2) was quantitatively determined by allowing the enzymatic reaction to go to completion. $IC_{50}$ values were obtained by determining the enzymatic rate at various inhibitor concentrations and plotted against inhibitor concentration, followed by a hyperbolic saturation curve fit. The data used for the saturation curves were performed in duplicate or triplicate, depending on the quality of the data.

**Fluorescence Iron Binding Assay.** Fluorescence readings were taken with a Perkin-Elmer luminescence spectrometer LS 50 B in the presence and absence of iron with the excitation maximum $\lambda_{ex}$ = 360 nm and the emission maximum $\lambda_{em}$ = 410 nm. Excitation slit was set at 5 nm, and the emission slit was set at 10 nm. Because of the low intensity of the fluorophore, the filter was kept open. As a control, 1 mM 8-HQ-5-sulfonic acid was dissolved in 25 mM HEPES buffer (pH 8.5) and aliquoted to a 2 mL cuvette. In a separate cuvette, 1 mM 8-HQ-5-sulfonic acid and either 10 $\mu$M $Fe^{2+}$ (as $[NH_4]_2[Fe][SO_4]_2 \cdot 6H_2O$) or $Fe^{3+}$ (as $Fe_2(SO_4)_3$) in 25 mM HEPES buffer (pH 8.5) was added and allowed to equilibrate for 5 min. For the experimental, 2 mL of 1 mM **1** was dissolved in 25 mM HEPES buffer (pH 8.5) and the fluorescence intensity taken. In a separate cuvette, 1 mM **1** was dissolved in 25 mM HEPES buffer (pH 8.5) and was incubated with less than 1 $\mu$M (by iron content) of 12-LOX and allowed to equilibrate for 5 min.

*DPPH Antioxidant Test.* Compound **1** was dissolved in dimethyl sulfoxide (DMSO) at 1−20 mM concentration (1000-fold concentrated). The antioxidant activity of this compound was assayed by monitoring the quenching of the standard free radical 1,1-diphenyl-2-picrylhydrazyl (DPPH) upon reaction with the testing compounds.[89,90] A known free radical scavanger, nordihydroguaiaretic acid (NDGA) was used as a positive control. Then 10 $\mu$L of the testing reagent (1 mM), to achieve a final concentration of 5 $\mu$M, was added to 2 mL of 500 $\mu$M DPPH, stirring in a cuvette. Optical absorbance was monitored and recorded at 25 s intervals as described elsewhere.[89,90] The decrease in optical absorbance at 517 nm was monitored using a Perkin-Elmer Lambda 40 spectrometer. The rate of reaction is proportional to the antioxidant potency of the test compounds.

*Steady-State Inhibition Kinetics.* Lipoxygenase rates were determined by monitoring the formation of the conjugated product, 12-HPETE, at 234 nm ($\varepsilon$ = 25 000 $M^{-1}$ $cm^{-1}$) with a Perkin-Elmer Lambda 40 UV/vis spectrophotometer. Reactions were initiated by adding approximately 80 nM 12-LOX to a constantly stirring 2 mL cuvette containing 3−40 $\mu$M AA in 25 mM HEPES buffer (pH 7.5), in the presence of 0.01% Triton X-100. The substrate concentration was quantitated by allowing the enzymatic reaction to proceed to completion. Kinetic data were obtained by recording initial enzymatic rates, at varied inhibitor concentrations, and subsequently fitted to the Henri−Michaelis−Menten equation, using KaleidaGraph (Synergy) to determine the microscopic rate constants, $V_{max}$ ($\mu$mol/min/mg) and $V_{max}/K_M$ ($\mu$mol/min/mg/$\mu$M). These rate constants were subsequently replotted and normalized to the iron content (120 nM) as $1/k_{cat}$ and $K_M/k_{cat}$, versus inhibitor concentration, to yield $K_{iu}$ and $K_{ic}$, respectively.

*Incubation Inhibition Kinetics.* 12-LOX rates were determined as above, with the following modifications. First, 1 $\mu$L of 1 mM compound **2**, in DMSO, was added to 30 $\mu$L of 12-LOX (approximately 5 $\mu$M), and allowed to sit on ice for intervals of 2 min, upward to 10 min. Then the mixture was added at designated time periods to a constantly stirring 2 mL cuvette, containing 10 $\mu$M AA in 25 mM HEPES buffer (pH 8.0), in the presence of 0.01% Triton X-100. The control to this reaction was the same as above, but only DMSO was added. Incubated samples with inhibitor were also dialyzed to demonstrate reversible inhibition, but the enzyme died in the 2 h time frame of the experiment.

*Cyclooxygenase Assay.* Ovine COX-1 (catalogue no. 60100) and human COX-2 (catalogue no. 60122) were purchased from Cayman chemical. Approximately 2 $\mu$g of either COX-1 or COX-2 were added to buffer containing 100 $\mu$M AA, 0.1 M Tris-HCl buffer (pH 8.0), 5 mM EDTA, 2 mM phenol, and 1 $\mu$M hematin at 37 °C. Data was collected using a Hansatech DW1 oxygen electrode chamber. Inhibitors were incubated with the respective COX for 20 min and added to the reaction mixture, and the consumption of oxygen was recorded. Ibuprofen and the carrier solvent, DMSO, were used as positive and negative controls, respectively.

*Mouse 12/15-Lipoxygenase Expression, Purification and $IC_{50}$ Assay.* 12/15-mouse lipoxygenase (12/15-LOX), with an N-terminus His-tag was expressed in SF9 insect cells. 12/15-LOX was PCR amplified from the pGFP-ALOX15 vector (Gift of Dr. Jerry Nadler) using the following primers, 5′-GGCGCGCGTCGACATGCACCACCATCACCATCACTCACGGTGTCTACCGCATCCGCGTCTC-3′, 5′-GGCTCGAGTCTAGATCATTATATGGCCACGCTGTTTTCTACCAG-3′, yielding a fragment of approximately 2 kb. The PCR fragment was cut with SalI and XhoI and ligated into a pFastBac1 vector, cut with the same enzymes. 12/15LOX-pFastBac was then transposed into a recombinant pFastBac bacmid using DH10Bac cells and transfected into SF9 cells, as described in the product literature for pFastBac1. For purification, infected SF9 cells were harvested after 72 h by centrifugation and stored at −20 °C. Thawed cells were dounced in 25 mM HEPES pH 7.5, and extract was loaded onto a Bio Rad UNO Q1 ion exchange column. 12/15-mLO was eluded with a 0−1 M sodium chloride linear gradient using 25 mM HEPES running buffer. Glycerol was added (15%) to active fractions, which were stored at −80 °C. It should be noted that the His-tag purification method could not be used due to rapid inactivation of the protein. It was unclear as to the cause of this inactivation, but it appears that certain salts lead to the inactivation. Inhibitor assays were

performed on a Perkin-Elmer Lambda 45 UV/vis spectrophotometer. Assay buffer consisted of 10 $\mu$M arachidonic acid added to 25 mM HEPES (pH 7.5). These assays were performed in the absence of Triton X-100 because it was found to inactivate 12/15-LOX. 12/15-LOX was defrosted on ice and added to the cuvette containing substrate and inhibitor. Conjugated product formation was monitored at 234 nm. The one-point inhibition percentage for weak inhibitors was calculated as 1 − (maximal experimental rate/maximal control rate) × 100%. The multipoint $IC_{50}$ value was determined by plotting the percent inhibition vs [inhibitor] and fitting with a hyperbolic equation, as defined before.[70]

*Cellular Inhibition Assay.* To determine if these compounds were effective in a cellular environment, a select few were tested against 12-LOX in platelets. Human platelets were obtained from healthy volunteers at Thomas Jefferson University, and this study was approved by the Thomas Jefferson University Institutional Review Board. Informed consent was obtained from all donors prior to blood draw. First, 20 mL of blood was drawn and centrifuged at 200*g* for 15 min at room temperature. Then to the plasma, 10% ACD (1:10) and Apyrase (1 $\mu$L/2.5 mL) were added and the solution centrifuged at 2000*g* for 15 min at room temperature. The platelets were resuspended with Tyrode's buffer and adjusted to a concentration of $3.0 \times 10^8$ platelets/mL. The platelets were subsequently treated with inhibitor for 10 min at 37 °C prior to stimulation with 20 $\mu$M PAR1-AP (SFLLRN) under stirring conditions in an aggregometer. Following aggregation, samples were centrifuged at 2000*g* for 10 min, the supernatant transferred to scintillation vials, extracted with methylene chloride, reduced with triphenylphosphine, and evaporated to dryness. The dry samples were then resuspended in methanol and stored at −20 °C until analyzed by Finnigan LTQ liquid chromatography−tandem mass spectrometry (LC−MS/MS) system. An internal control, 12-deuterated($d_8$)- HETE (12-$d_8$-HETE) was added to each sample prior to injection on LC-MS to account for the variation in the detector response, it was assumed that the detector response for 12-HETE and 12-$d_8$-HETE would be similar. A Thermo Electron Corp. Aquasil (3 $\mu$m, 100 mm × 2.1 mm) C-18 column was used to detect the HETEs with an elution protocol consisting of 0.2 mL/min flow rate and a linear gradient from 54.9% MeCN, 45% $H_2O$, and 0.1% THF to 69.9% MeCN, 30% $H_2O$, and 0.1% THF. The corresponding 12-HETE and 12-$d_8$-HETE compounds were detected using selective ion monitoring analysis ($m/z$ =318.7 to 319.7 and 326.8 to 327.7) in negative ion mode and then identified by fragmentation pattern (12-HETE, parent ion at $m/z$ 319 and fragments at $m/z$ 179 and 163; 12-$d_8$-HETE, parent ion at $m/z$ 327 and fragments at $m/z$ 184 and 214) from MS−MS.[91] The electrospray voltage was set to 5.0 kV, and a global acquisition MS mode was used. The MS−MS scan was performed for the five most abundant precursor ions. The collision induced dissociation (CID) was used for MS-MS with a collision energy of 35 eV. The peak intensities of 12-HETEs were normalized to the 12-$d_8$-HETE intensities. The amount of 12-HETE in samples was estimated using a standard curve generated from pure 12-HETE with concentrations ranging from 0 to 2.5 $\mu$M along with a constant amount of 12-$d_8$-HETE added in each sample. The assay is linear in the concentration range used for the 12-HETE standard curve with a $R^2$ value of 0.997.

*Inhibition of 12-HETE Production in Human Donor Islets.* Studies with human donor islets had institutional approval. Islets were obtained from the Integrated Islet Distribution Program. Human donor islets were incubated overnight in CMRL media (catalogue no. 15−110-CV Media-Tech, Inc. Manassas, VA) containing 10% fetal bovine serum + pen/strep. The islets were serum-starved by incubating in serum free media, CMRL containing pen/strep and 1% fatty acid free human serum albumin (catalogue no. A1887 Sigma, St. Louis, MO) for 1 h. Islets were incubated in serum-free media containing 100 $\mu$M arachadonic acid (catalogue no. BML-FA003−0100, Enzo Life Sciences Plymouth Meeting, PA), with and without 10 $\mu$M of compound **1** for 60 min at 37 °C. Calcium ionophore, 5 $\mu$M of A23187 (catalogue no. C7522, Sigma, St. Louis, MO), was added for an additional 30 min. Samples were harvested, centrifuged at 1000 rpm for 5 min, and supernatant drawn off and islet pellet stored at −80 °C. Cell pellets were extracted using $CHCl_3$/MeOH and samples dried under nitrogen gas before reconstitution in 250 $\mu$L of ELISA sample buffer. 12-HETE levels in samples were determined using a 12-HETE ELISA kit (catalogue no. 901−050, Assay Design, Plymouth Meeting, PA).

## ■ ASSOCIATED CONTENT

**Ⓢ Supporting Information.** Additional experimental procedures and spectroscopic data ($^1$H NMR, LC/MS, and HRMS) for representative compounds. Analytical methods for the chiral HPLC separation of enantiomers and kinetic inhibition data are also included. This material is available free of charge via the Internet at http://pubs.acs.org.

## ■ AUTHOR INFORMATION

### Corresponding Author

*For D.J.M.: phone, 301-217-4381; fax, 301-217-5736; E-mail, maloneyd@mail.nih.gov. For T.R.H: phone, 831-459-5884; fax, 831-459-2935; E-mail: holman@ucsc.edu.

### Present Addresses

#Department of Molecular Medicine, Beckman Research Institute at City of Hope, 1500 East Duarte Road, Duarte, California 91010-3000, United States.

### Author Contributions

⊥Both of these authors contributed equally to this work.

## ■ ACKNOWLEDGMENT

We thank Eric Hoobler for the 5-LOX assay, Norine Kuhn for islet incubations and the 12-HETE ELISA, Sam Michael for assistance with the primary HTP screen, and Paul Shinn and Danielle vanLeer for assistance with compound management and purification. We also thank Christina Greco for critical reading of the manuscript. Financial support was from the National Institutes of Health (R01 GM56062 (T.R.H.), R00 HL089457 (M.H.), R01 DK 55240 (D.T.F., J.L.N.)), the Juvenile Diabetes Research Foundation (D.T.F., T.R.H., J.L.N.), and the Molecular Libraries Initiative of the National Institutes of Health Roadmap for Medical Research (R03 MH081283 (T.R.H.)). Additional financial support was from NIH (S10-RR20939 (T.R.H.)) and the California Institute for Quantitative Biosciences (T.R.H.) for the UCSC MS Facility.

## ■ ABBREVIATIONS USED

LOX, lipoxygenase; soybean LOX-1, soybean lipoxygenase-1; 15-LOX-1, human reticulocyte 15-lipoxygenase-1; 15-LOX-2, human epithelial 15-lipoxygenase-2; 12-LOX, human platelet-type 12-lipoxygenase; rabbit 15-LOX, rabbit reticulocyte 15-lipoxygenase; COX, cyclooxygenase; NDGA, nordihydroguaiaretic acid; AA, arachidonic acid; 15-HPETE, 15-(*S*)-hydroperoxyeicosatetraenoic acid; 15-HETE, 15-(*S*)-hydroxyeicosatetraenoic acid; 12-HPETE, 12-(*S*)-hydroperoxyeicosatetraenoic acid; 12-HETE, 12-(*S*)-hydroxyeicosatetraenoic acid; LA, linoleic acid; 13-HPODE, 13-(*S*)-hydroperoxyoctadecadienoic acid; 13-HODE, 13-(*S*)-hydroxyoctadecadienoic acid; ALA, α-linolenic acid; 13-HPOTrE, 13-(*S*)-hydroperoxyoctadecatrienoic acid; 8-HQ, 8-hydroxyquinoline; mRNA, messenger ribonucleic acid; $V_{max}$, maximal velocity (mmol/min); $k_{cat}$, first-order catalytic rate constant ($V_{max}$/[E]

($s^{-1}$)); $K_M$, Henri−Michaelis−Menten Constant (mM); [E], total active enzyme concentration; $IC_{50}$, inhibitor constant at 50% inhibition; DPPH, 1.1-diphenyl-2-picrylhydrazyl; XO, xylenol orange; HTS, high-throughput screening; MLSMR, Molecular Libraries Small Molecule Repository; qHTS, quantitative high-throughput screening; CRC, concentration−response curve; SD, standard deviation; MLPCN, Molecular Libraries Probe Production Center Network

## REFERENCES


(1) Solomon, E. I.; Zhou, J.; Neese, F.; Pavel, E. G. New Insights from Spectroscopy into the Structure/Function Relationships of Lipoxygenases. *Chem. Biol.* **1997**, *4*, 795–808.

(2) Ford-Hutchinson, A. W.; Gresser, M.; Young, R. N. 5-Lipoxygenase. *Annu. Rev. Biochem.* **1994**, *63*, 383–417.

(3) Kuhn, H.; Chaitidis, P.; Roffeis, J.; Walther, M. Arachidonic Acid Metabolites in the Cardiovascular System: The Role of Lipoxygenase Isoforms in Atherogenesis with Particular Emphasis on Vascular Remodeling. *J. Cardiovasc. Pharmacol.* **2007**, *50*, 609–620.

(4) Pace-Asciak, C. R.; Asotra, S. Biosynthesis, Catabolism, and Biological Properties of HPETES, Hydroperoxide Derivatives of Arachidonic Acid. *Free Radical Biol. Med.* **1989**, *7*, 409–433.

(5) Radmark, O.; Samuelsson, B. 5-Lipoxygenase: Regulation and Possible Involvement in Atherosclerosis. *Prostaglandins Other Lipid Mediators* **2007**, *83*, 162–174.

(6) Brock, T. G. Regulating Leukotriene Synthesis: The Role of Nuclear 5-Lipoxygenase. *J. Cell. Biochem.* **2005**, *96*, 1203–1211.

(7) Newcomer, M. E.; Gilbert, N. C. Location, Location, Location: Compartmentalization of Early Events in Leukotriene Biosynthesis. *J. Biol. Chem.* **2010**, *285*, 25109–25114.

(8) Ghosh, J. Inhibition of Arachidonate 5-Lipoxygenase Triggers Prostate Cancer Cell Death through Rapid Activation of C-Jun N-Terminal Kinase. *Biochem. Biophys. Res. Commun.* **2003**, *307*, 342–349.

(9) Ghosh, J.; Myers, C. E. Inhibition of Arachidonate 5-Lipoxygenase Triggers Massive Apoptosis in Human Prostate Cancer Cells. *Proc. Natl. Acad. Sci. U.S.A.* **1998**, *95*, 13182–13187.

(10) Nakano, H.; Inoue, T.; Kawasaki, N.; Miyataka, H.; Matsumoto, H.; Taguchi, T.; Inagaki, N.; Nagai, H.; Satoh, T. Synthesis and Biological Activities of Novel Antiallergic Agents with 5-Lipoxygenase Inhibiting Action. *Bioorg. Med. Chem.* **2000**, *8*, 373–380.

(11) Radmark, O.; Werz, O.; Steinhilber, D.; Samuelsson, B. 5-Lipoxygenase: Regulation of Expression and Enzyme Activity. *Trends Biochem. Sci.* **2007**, *32*, 332–341.

(12) Berger, W.; De Chandt, M. T.; Cairns, C. B. Zileuton: Clinical Implications of 5-Lipoxygenase Inhibition in Severe Airway Disease. *In.t J. Clin. Pract.* **2007**, *61*, 663–676.

(13) Masferrer, J. L.; Zweifel, B. S.; Hardy, M.; Anderson, G. D.; Dufield, D.; Cortes-Burgos, L.; Pufahl, R. A.; Graneto, M. Pharmacology of Pf-4191834, a Novel, Selective Non-Redox 5-Lipoxygenase Inhibitor Effective in Inflammation and Pain. *J. Pharmacol. Exp. Ther.* **2010**, *334*, 294–301.

(14) Ducharme, Y.; Blouin, M.; Brideau, C.; Chateauneuf, A.; Gareau, Y.; Grimm, E. L.; Juteau, H.; Laliberte, S.; MacKay, B.; Masse, F.; Ouellet, M.; Salem, M.; Styhler, A.; Friesen, R. W. The Discovery of Setileuton, a Potent and Selective 5-Lipoxygenase Inhibitor. *ACS Med. Chem. Lett.* **2010**, *1*, 170–174.

(15) Company information: www.pfizer.com, www.merck.com.

(16) Jones, R.; Adel-Alvarez, L. A.; Alvarez, O. R.; Broaddus, R.; Das, S. Arachidonic Acid and Colorectal Carcinogenesis. *Mol. Cell. Biochem.* **2003**, *253*, 141–149.

(17) Shureiqi, I.; Lippman, S. M. Lipoxygenase Modulation to Reverse Carcinogenesis. *Cancer Res.* **2001**, *61*, 6307–6312.

(18) Kelavkar, U. P.; Cohen, C.; Kamitani, H.; Eling, T. E.; Badr, K. F. Concordant Induction of 15-Lipoxygenase-1 and Mutant P53 Expression in Human Prostate Adenocarcinoma: Correlation with Gleason Staging. *Carcinogenesis* **2000**, *21*, 1777–1787.

(19) Hsi, L. C.; Wilson, L. C.; Eling, T. E. Opposing Effects of 15-Lipoxygenase-1 and -2 Metabolites on Mapk Signaling in Prostate Alteration in Peroxisome Proliferator-Activated Receptor Gamma. *J. Biol. Chem.* **2002**, *277*, 40549–40556.

(20) Shappell, S. B.; Manning, S.; Boeglin, W. E.; Guan, Y. F.; Roberts, R. L.; Davis, L.; Olson, S. J.; Jack, G. S.; Coffey, C. S.; Wheeler, T. M.; Breyer, M. D.; Brash, A. R. Alterations in Lipoxygenase and Cyclooxygenase-2 Catalytic Activity and MRNA Expression in Prostate Carcinoma. *Neoplasia* **2001**, *3*, 287–303.

(21) Shappell, S. B.; Olson, S. J.; Hannah, S. E.; Manning, S.; Roberts, R. L.; Masumori, N.; Jisaka, M.; Boeglin, W. E.; Vader, V.; Dave, D. S.; Shook, M. F.; Thomas, T. Z.; Funk, C. D.; Brash, A. R.; Matusik, R. J. Elevated Expression of 12/15-Lipoxygenase and Cyclooxygenase-2 in a Transgenic Mouse Model of Prostate Carcinoma. *Cancer Res.* **2003**, *63*, 2256–2267.

(22) Brash, A. R.; Boeglin, W. E.; Chang, M. S. Discovery of a Second 15s-Lipoxygenase in Humans. *Proc. Natl. Acad. Sci. U.S.A.* **1997**, *94*, 6148–6152.

(23) Gonzalez, A. L.; Roberts, R. L.; Massion, P. P.; Olson, S. J.; Shyr, Y.; Shappell, S. B. 15-Lipoxygenase-2 Expression in Benign and Neoplastic Lung: An Immunohistochemical Study and Correlation with Tumor Grade and Proliferation. *Hum. Pathol.* **2004**, *35*, 840–849.

(24) Suraneni, M. V.; Schneider-Broussard, R.; Moore, J. R.; Davis, T. C.; Maldonado, C. J.; Li, H.; Newman, R. A.; Kusewitt, D.; Hu, J.; Yang, P.; Tang, D. G. Transgenic Expression of 15-Lipoxygenase 2 (15-Lox2) in Mouse Prostate Leads to Hyperplasia and Cell Senescence. *Oncogene* **2010**, *29*, 4261–4275.

(25) Tang, D. G.; Bhatia, B.; Tang, S.; Schneider-Broussard, R. 15-Lipoxygenase 2 (15-Lox2) Is a Functional Tumor Suppressor That Regulates Human Prostate Epithelial Cell Differentiation, Senescence, and Growth (Size). *Prostaglandins Other Lipid Mediators* **2007**, *82*, 135–146.

(26) Jobard, F.; Lefevre, C.; Karaduman, A.; Blanchet-Bardon, C.; Emre, S.; Weissenbach, J.; Ozguc, M.; Lathrop, M.; Prud'homme, J. F.; Fischer, J. Lipoxygenase-3 (Aloxe3) and 12(*R*)-Lipoxygenase (Alox12b) Are Mutated in Non-Bullous Congenital Ichthyosiform Erythroderma (Ncie) Linked to Chromosome 17p13.1. *Hum. Mol. Genet.* **2002**, *11*, 107–113.

(27) Hussain, H.; Shornick, L. P.; Shannon, V. R.; Wilson, J. D.; Funk, C. D.; Pentland, A. P.; Holtzman, M. J. Epidermis Contains Platelet-Type 12-Lipoxygenase That Is Overexpressed in Germinal Layer Keratinocytes in Psoriasis. *Am. J. Physiol.* **1994**, *266*, C243–C253.

(28) Ding, X. Z.; Iversen, P.; Cluck, M. W.; Knezetic, J. A.; Adrian, T. E. Lipoxygenase Inhibitors Abolish Proliferation of Human Pancreatic Cancer Cells. *Biochem. Biophys. Res. Commun.* **1999**, *261*, 218–223.

(29) Connolly, J. M.; Rose, D. P. Enhanced Angiogenesis and Growth of 12-Lipoxygenase Gene-Transfected Mcf-7 Human Breast Cancer Cells in Athymic Nude Mice. *Cancer Lett.* **1998**, *132*, 107–112.

(30) Natarajan, R.; Nadler, J. Role of Lipoxygenases in Breast Cancer. *Front. Biosci.* **1998**, *3*, E81–E88.

(31) Ma, K.; Nunemaker, C. S.; Wu, R.; Chakrabarti, S. K.; Taylor-Fishwick, D. A.; Nadler, J. L. 12-Lipoxygenase Products Reduce Insulin Secretion and {Beta}-Cell Viability in Human Islets. *J. Clin. Endocrinol. Metab.* **2010**, *95*, 887–893.

(32) Thomas, C. P.; Morgan, L. T.; Maskrey, B. H.; Murphy, R. C.; Kuhn, H.; Hazen, S. L.; Goodall, A. H.; Hamali, H. A.; Collins, P. W.; O'Donnell, V. B. Phospholipid-Esterified Eicosanoids Are Generated in Agonist-Activated Human Platelets and Enhance Tissue Factor-Dependent Thrombin Generation. *J. Biol. Chem.* **2010**, *285*, 6891–6903.

(33) Holinstat, M.; Boutaud, O.; Apopa, P. L.; Vesci, J.; Bala, M.; Oates, J. A.; Hamm, H. E. Protease-Activated Receptor Signaling in Platelets Activates Cytosolic Phospholipase A2alpha Differently for Cyclooxygenase-1 and 12-Lipoxygenase Catalysis. *Arterioscler. Thromb. Vasc. Biol.* **2011**, *31*, 435–442.

(34) Kaur, G.; Jalagadugula, G.; Mao, G.; Rao, A. K. Runx1/Core Binding Factor A2 Regulates Platelet 12-Lipoxygenase Gene (Alox12): Studies in Human Runx1 Haplodeficiency. *Blood* **2010**, *115*, 3128–3135.

(35) Catalano, A.; Procopio, A. New Aspects on the Role of Lipoxygenases in Cancer Progression. *Histol. Histopathol.* **2005**, *20*, 969–975.

(36) Krishnamoorthy, S.; Jin, R.; Cai, Y.; Maddipati, K. R.; Nie, D.; Pages, G.; Tucker, S. C.; Honn, K. V. 12-Lipoxygenase and the Regulation of Hypoxia-Inducible Factor in Prostate Cancer Cells. *Exp. Cell Res.* **2010**, *316*, 1706–1715.

(37) Steele, V. E.; Holmes, C. A.; Hawk, E. T.; Kopelovich, L.; Lubet, R. A.; Crowell, J. A.; Sigman, C. C.; Kelloff, G. J. Lipoxygenase Inhibitors as Potential Cancer Chemopreventives. *Cancer Epidemiol., Biomarkers Prev.* **1999**, *8*, 467–483.

(38) Jiang, W. G.; Douglas-Jones, A.; Mansel, R. E. Levels of Expression of Lipoxygenases and Cyclooxygenase-2 in Human Breast Cancer. *Prostaglandins, Leukotrienes Essent. Fatty Acids* **2003**, *69*, 275–281.

(39) Mohammad, A. M.; Abdel, H. A.; Abdel, W.; Ahmed, A. M.; Wael, T.; Eiman, G. Expression of Cyclooxygenase-2 and 12-Lipoxygenase in Human Breast Cancer and Their Relationship with Her-2/Neu and Hormonal Receptors: Impact on Prognosis and Therapy. *Indian .J Cancer* **2006**, *43*, 163–168.

(40) Zeeneldin, A. A.; Mohamed, A. M.; Abdel, H. A.; Taha, F. M.; Goda, I. A.; Abodeef, W. T. Survival Effects of Cyclooxygenase-2 and 12-Lipooxygenase in Egyptian Women with Operable Breast Cancer. *Indian J. Cancer* **2009**, *46*, 54–60.

(41) Agrawal, V. K.; Bano, S.; Khadikar, P. V. Qsar Study on 5-Lipoxygenase Inhibitors Using Distance-Based Topological Indices. *Bioorg. Med. Chem.* **2003**, *11*, 5519–5527.

(42) Arockia Babu, M.; Shakya, N.; Prathipati, P.; Kaskhedikar, S. G.; Saxena, A. K. Development of 3d-QSAR Models for 5-Lipoxygenase Antagonists: Chalcones. *Bioorg. Med. Chem.* **2002**, *10*, 4035–4041.

(43) Basha, A.; Ratajczyk, J. D.; Dyer, R. D.; Young, P.; Carter, G. W.; Brooks, C. D. W. Structure−Activity Relationships of Pyrimido-Pyrimidine Series of 5-Lipoxygenase Inhibitors. *Med. Chem. Res.* **1996**, *6*, 61–67.

(44) Fleiseher, R.; Frohberg, P.; Buge, A.; Nuhn, P.; Wiese, M. QSAR Analysis of Substituted 2-Phenylhydrazonoacetamides Acting as Inhibitors of 15-Lipoxygenase. *Quant. Struct.−Act. Relationships* **2000**, *19*, 162–172.

(45) Kim, K. H.; Martin, Y. C.; Brooks, C. D. W. Quantitative Structure−Activity Relationships of 5-Lipoxygenase Inhibitors Inhibitory Potency of Triazinone Analogues in a Broken Cell. *Quant. Struct.−Activity Relationships* **1996**, *15*, 491–497.

(46) Kim, K. H.; Martin, Y. C.; Brooks, D. W.; Dyer, R. D.; Carter, G. W. Quantitative Structure−Activity Relationships of 5-Lipoxygenase Inhibitors Inhibitory Potency of Pyridazinone Analogues. *J. Pharm. Sci.* **1994**, *83*, 433–438.

(47) Mano, T.; Stevens, R. W.; Ando, K.; Nakao, K.; Okumura, Y.; Sakakibara, M.; Okumura, T.; Tamura, T.; Miyamoto, K. Novel Imidazole Compounds as a New Series of Potent, Orally Active Inhibitors of 5-Lipoxygenase. *Bioorg. Med. Chem.* **2003**, *11*, 3879–3887.

(48) Redrejo-Rodriguez, M.; Tejeda-Cano, A.; Pinto, M. D.; Macias, P. Lipoxygenase Inhibition by Flavonoids: Semiempirical Study of the Structure−Activity Relation. *J. Mol. Struct.—THEOCHEM* **2004**, *674*, 121–124.

(49) Stewart, A. O.; Bhatia, P. A.; Martin, J. G.; Summers, J. B.; Rodriques, K. E.; Martin, M. B.; Holms, J. H.; Moore, J. L.; Craig, R. A.; Kolasa, T.; Ratajczyk, J. D.; Mazdiyasni, H.; Kerdesky, F. A.; DeNinno, S. L.; Maki, R. G.; Bouska, J. B.; Young, P. R.; Lanni, C.; Bell, R. L.; Carter, G. W.; Brooks, C. D. Structure−Activity Relationships of *N*-Hydroxyurea 5-Lipoxygenase Inhibitors. *J. Med. Chem.* **1997**, *40*, 1955–1968.

(50) Amagata, T.; Whitman, S.; Johnson, T. A.; Stessman, C. C.; Loo, C. P.; Lobkovsky, E.; Clardy, J.; Crews, P.; Holman, T. R. Exploring Sponge-Derived Terpenoids for Their Potency and Selectivity against 12-Human, 15-Human, and 15-Soybean Lipoxygenases. *J. Nat. Prod.* **2003**, *66*, 230–235.

(51) Benrezzouk, R.; Terencio, M. C.; Ferrandiz, M. L.; Hernandez-Perez, M.; Rabanal, R.; Alcaraz, M. J. Inhibition of 5-Lipoxygenase Activity by the Natural Anti-Inflammatory Compound Aethiopinone. *Inflammation Res.* **2001**, *50*, 96–101.

(52) Bracher, F.; Krauss, J.; Laufer, S. Effects of Natural Products Containing Acylresorcinol Partial Structures on Cyclooxygenases and 5-Lipoxygenase. *Pharmazie* **2001**, *56*, 430.

(53) Carroll, J.; Jonsson, E. N.; Ebel, R.; Hartman, M. S.; Holman, T. R.; Crews, P. Probing Sponge-Derived Terpenoids for Human 15-Lipoxygenase Inhibitors. *J. Org. Chem.* **2001**, *66*, 6847–6851.

(54) Fu, X.; Schmitz, F. J.; Govindan, M.; Abbas, S. A.; Hanson, K. M.; Horton, P. A.; Crews, P.; Laney, M.; Schatzman, R. C. Enzyme Inhibitors: New and Known Polybrominated Phenols and Diphenyl Ethers from Four Indo-Pacific Dysidea Sponges. *J. Nat. Prod.* **1995**, *58*, 1384–91.

(55) Jiang, Z. D.; Ketchum, S. O.; Gerwick, W. H. 5-Lipoxygenase-Derived Oxylipins from the Red Alga *Rhodymenia Pertusa*. *Phytochemistry* **2000**, *53*, 129–133.

(56) Rao, K. C. S.; Divakar, S.; Rao, A. G. A.; Karanth, N. G.; Suneetha, W. J.; Krishnakantha, T. P.; Sattur, A. P. Asperenone: An Inhibitor of 15-Lipoxygenase and of Human Platelet Aggregation from *Aspergillus Niger*. *Biotechnol. Lett.* **2002**, *24*, 1967–1970.

(57) Segraves, E. N.; Shah, R. R.; Segraves, N. L.; Johnson, T. A.; Whitman, S.; Sui, J. K.; Kenyon, V. A.; Cichewicz, R. H.; Crews, P.; Holman, T. R. Probing the Activity Differences of Simple and Complex Brominated Aryl Compounds against 15-Soybean, 15-Human, and 12-Human Lipoxygenase. *J. Med. Chem.* **2004**, *47*, 4060–4065.

(58) Suzuki, H.; Ueda, T.; Juranek, I.; Yamamoto, S.; Katoh, T.; Node, M.; Suzuki, T. Hinokitiol, a Selective Inhibitor of the Platelet-Type Isozyme of Arachidonate 12-Lipoxygenase. *Biochem. Biophys. Res. Commun.* **2000**, *275*, 885–889.

(59) Weinstein, D. S.; Liu, W.; Gu, Z.; Langevine, C.; Ngu, K.; Fadnis, L.; Combs, D. W.; Sitkoff, D.; Ahmad, S.; Zhuang, S.; Chen, X.; Wang, F. L.; Loughney, D. A.; Atwal, K. S.; Zahler, R.; Macor, J. E.; Madsen, C. S.; Murugesan, N. Tryptamine and Homotryptamine-Based Sulfonamides as Potent and Selective Inhibitors of 15-Lipoxygenase. *Bioorg. Med. Chem. Lett.* **2005**, *15*, 1435–1440.

(60) Deschamps, J. D.; Gautschi, J. T.; Whitman, S.; Johnson, T. A.; Gassner, N. C.; Crews, P.; Holman, T. R. Discovery of Platelet-Type 12-Human Lipoxygenase Selective Inhibitors by High-Throughput Screening of Structurally Diverse Libraries. *Bioorg. Med. Chem.* **2007**, *15*, 6900–6908.

(61) Vasquez-Martinez, Y.; Ohri, R. V.; Kenyon, V.; Holman, T. R.; Sepulveda-Boza, S. Structure−Activity Relationship Studies of Flavonoids as Potent Inhibitors of Human Platelet 12-LO, Reticulocyte 15-LO-1, and Prostate Epithelial 15-LO-2. *Bioorg. Med. Chem.* **2007**, *15*, 7408–7425.

(62) Yamamoto, S.; Katsukawa, M.; Nakano, A.; Hiraki, E.; Nishimura, K.; Jisaka, M.; Yokota, K.; Ueda, N. Arachidonate 12-Lipoxygenases with Reference to Their Selective Inhibitors. *Biochem. Biophys. Res. Commun.* **2005**, *338*, 122–127.

(63) Whitman, S.; Gezginci, M.; Timmermann, B. N.; Holman, T. R. Structure−Activity Relationship Studies of Nordihydroguaiaretic Acid Inhibitors toward Soybean, 12-Human, and 15-Human Lipoxygenase. *J. Med. Chem.* **2002**, *45*, 2659–2661.

(64) Deschamps, J. D.; Kenyon, V. A.; Holman, T. R. Baicalein Is a Potent in Vitro Inhibitor against Both Reticulocyte 15-Human and Platelet 12-Human Lipoxygenases. *Bioorg. Med. Chem.* **2006**, *14*, 4295–42301.

(65) Kenyon, V.; Chorny, I.; Carvajal, W. J.; Holman, T. R.; Jacobson, M. P. Novel Human Lipoxygenase Inhibitors Discovered Using Virtual Screening with Homology Models. *J. Med. Chem.* **2006**, *49*, 1356–1363.

(66) These compounds are a part of the NIH Small Molecule Repository: see http://mlsmr.glpg.com/MLSMR_HomePage/.

(67) Betti, M. General Condensation Reaction between B-Naphthol, Aldehydes and Amines. *Gazz. Chim. Ital.* **1900**, *30*, 310–316.

(68) Betti, M. General Condensation Reaction between B-Naphthol, Aldehydes and Amines. *Gazz. Chim. Ital.* **1901**, *31*, 377–393.

(69) Betti, M. General Condensation Reaction between B-Naphthol, Aldehydes and Amines. *Gazz. Chim. Ital.* **1901**, *31*, 170–184.

(70) Rai, G.; Kenyon, V.; Jadhav, A.; Schultz, L.; Armstrong, M.; Jameson, J. B.; Hoobler, E.; Leister, W.; Simeonov, A.; Holman, T. R.; Maloney, D. J. Discovery of Potent and Selective Inhibitors of Human Reticulocyte 15-Lipoxygenase-1. *J. Med. Chem.* **2010**, *53*, 7392–7404.

(71) Inglese, J.; Auld, D. S.; Jadhav, A.; Johnson, R. L.; Simeonov, A.; Yasgar, A.; Zheng, W.; Austin, C. P. Quantitative High-Throughput

Screening: A Titration-Based Approach That Efficiently Identifies Biological Activities in Large Chemical Libraries. *Proc. Natl. Acad. Sci. U.S.A.* **2006**, *103*, 11473–11478.

(72) Pierre, J. L.; Baret, P.; Serratrice, G. Hydroxyquinolines as Iron Chelators. *Curr. Med. Chem.* **2003**, *10*, 1077–1084.

(73) Liu, Z. D.; Kayyali, R.; Hider, R. C.; Porter, J. B.; Theobald, A. E. Design, Synthesis, and Evaluation of Novel 2-Substituted 3-Hydroxypyridin-4-Ones: Structure−Activity Investigation of Metalloenzyme Inhibition by Iron Chelators. *J. Med. Chem.* **2002**, *45*, 631–639.

(74) Nelson, M. J.; Brennan, B. A.; Chase, D. B.; Cowling, R. A.; Grove, G. N.; Scarrow, R. C. Structure and Kinetics of Formation of Catechol Complexes of Ferric Soybean Lipoxygenase-1. *Biochemistry* **1995**, *34*, 15219–15229.

(75) Hahn, C.; Sieler, J.; Taube, R. Synthesis of 2,6-Bis-(diphenylphosphinomethyl)pyridine-monoligand−Rhodium(I) Complexes [Rh(Pnp)L]X with L = Pyridine, Ch3cn, Dmso and X = Cf3so3, Bf4 from the Corresponding Ethylene Complex and Comparison of the Structures to the Piperidine Complex (L = Piperidine, X = Bf4). *Polyhedron* **1998**, *17*, 1183–1193.

(76) Gupta, A. K.; Bluhm, R. Seborrheic Dermatitis. *J. Eur. Acad. Dermatol. Venereol.* **2004**, *18*, 13–26quiz 19−20.

(77) Kemal, C.; Louis-Flamberg, P.; Krupinski-Olsen, R.; Shorter, A. L. Reductive Inactivation of Soybean Lipoxygenase 1 by Catechols: A Possible Mechanism for Regulation of Lipoxygenase Activity. *Biochemistry* **1987**, *26*, 7064–7072.

(78) McMillan, R. M.; Walker, E. R. Designing Therapeutically Effective 5-Lipoxygenase Inhibitors. *Trends Pharmacol. Sci.* **1992**, *13*, 323–330.

(79) McGovern, S. L.; Helfand, B. T.; Feng, B.; Shoichet, B. K. A Specific Mechanism of Nonspecific Inhibition. *J. Med. Chem.* **2003**, *46*, 4265–4272.

(80) Cornish-Bowden, A. *Fundamentals of Enzyme Kinetics*; Portland Press, Ltd.: Colchester, UK, 1995; p 343.

(81) Crichlow, G. V.; Lubetsky, J. B.; Leng, L.; Bucala, R.; Lolis, E. J. Structural and Kinetic Analyses of Macrophage Migration Inhibitory Factor Active Site Interactions. *Biochemistry* **2009**, *48*, 132–139.

(82) Sloane, D.; Leung, R.; Barnett, J.; Craik, C.; Sigal, E. Conversion of Human 15-Lipoxygenase to an Efficient 12-Lipoxygenase—the Side-Chain Geometry of Amino Acids 417 and 418 Determine Positional Specificity. *Protein Eng.* **1995**, *8*, 275–282.

(83) McLean, L. R.; Zhang, Y.; Li, H.; Li, Z.; Lukasczyk, U.; Choi, Y. M.; Han, Z.; Prisco, J.; Fordham, J.; Tsay, J. T.; Reiling, S.; Vaz, R. J.; Li, Y. Discovery of Covalent Inhibitors for Mif Tautomerase via Cocrystal Structures with Phantom Hits from Virtual Screening. *Bioorg. Med. Chem. Lett.* **2009**, *19*, 6717–6720.

(84) Gilbert, A. M.; Bursavich, M. G.; Lombardi, S.; Georgiadis, K. E.; Reifenberg, E.; Flannery, C. R.; Morris, E. A. *N*-((8-Hydroxy-5-substituted-quinolin-7-Yl)(phenyl)methyl)-2-phenyloxy/Amin *O*-Acetamide Inhibitors of Adamts-5 (Aggrecanase-2). *Bioorg. Med. Chem. Lett.* **2008**, *18*, 6454–6457.

(85) Ohri, R. V.; Radosevich, A. T.; Hrovat, K. J.; Musich, C.; Huang, D.; Holman, T. R.; Toste, F. D. A Re(V)-Catalyzed C−N Bond-Forming Route to Human Lipoxygenase Inhibitors. *Org. Lett.* **2005**, *7*, 2501–2504.

(86) Chen, X.-S.; Brash, A.; Funk, C. Purification and Characterization of Recombinant Histidine-Tagged Human Platelet 12-Lipoxygenase Expressed in a Baculovirus/Insect Cell System. *Eur. J. Biochem.* **1993**, *214*, 845–852.

(87) Robinson, S. J.; Hoobler, E. K.; Riener, M.; Loveridge, S. T.; Tenney, K.; Valeriote, F. A.; Holman, T. R.; Crews, P. Using Enzyme Assays to Evaluate the Structure and Bioactivity of Sponge-Derived Meroterpenes. *J. Nat. Prod.* **2009**, *72*, 1857–1863.

(88) Michael, S.; Auld, D.; Klumpp, C.; Jadhav, A.; Zheng, W.; Thorne, N.; Austin, C. P.; Inglese, J.; Simeonov, A. A Robotic Platform for Quantitative High-Throughput Screening. *Assay Drug Dev. Technol.* **2008**, *6*, 637–657.

(89) van Leyen, K.; Arai, K.; Jin, G.; Kenyon, V.; Gerstner, B.; Rosenberg, P. A.; Holman, T. R.; Lo, E. H. Novel Lipoxygenase Inhibitors as Neuroprotective Reagents. *J. Neurosci. Res.* **2008**, *86*, 904–909.

(90) Wang, H.; Li, J.; Follett, P. L.; Zhang, Y.; Cotanche, D. A.; Jensen, F. E.; Volpe, J. J.; Rosenberg, P. A. 12-Lipoxygenase Plays a Key Role in Cell Death Caused by Glutathione Depletion and Arachidonic Acid in Rat Oligodendrocytes. *Eur. J. Neurosci.* **2004**, *20*, 2049–2058.

(91) Kim, H. Y.; Sawazaki, S. Structural Analysis of Hydroxy Fatty Acids by Thermospray Liquid Chromatography/Tandem Mass Spectrometry. *Biol. Mass Spectrom.* **1993**, *22*, 302–310.